Electronic Supplementary Information for:

Catalytic Dinitrogen Reduction to Hydrazine and Ammonia using $Cr(N_2)_2(diphosphine)_2$ Complexes

Charles H. Beasley,[‡] Olivia L. Duletski,[‡] Ksenia S. Stankevich,[‡] Navamoney Arulsamy,[†] and Michael T. Mock[‡]*

[‡]Department of Chemistry and Biochemistry, Montana State University, Bozeman, Montana 59715, United States

[†]Department of Chemistry, University of Wyoming, Laramie, Wyoming 82071, United States

Table of Contents

General Procedures

NMR spectra were recorded at 298 K on a Bruker ASCEND AVANCE III HD 500 MHz (500.2 MHz for ^{1}H, 125.8 MHz for ^{13}C, and 50.0 MHz for ^{15}N NMR spectroscopy) spectrometer equipped with a Prodigy (liquid nitrogen cooled) cryoprobe, or a Bruker AVANCE NEO 400 MHz (400.1 MHz for ^{1}H NMR spectroscopy, 40.5 MHz for ^{15}N NMR spectroscopy) spectrometer. ^{1}H and ^{13}C NMR spectra were referenced to residual proton resonances in deuterated solvent. ^{15}N NMR chemical shifts were referenced to CH_3NO_2 (0 ppm). Elemental Analysis was performed by Atlantic Microlabs, Norcross, GA.

Infrared spectra were recorded on a Thermo Scientific Nicolet iS50 FT-IR spectrometer at ambient temperature and under a purge stream of nitrogen gas. In situ IR experiments were performed in a fume hood using a N_2 purge from a Schlenk line manifold and recorded on a Mettler-Toledo ReactIR 15 spectrometer equipped with a liquid-nitrogen-cooled MCT detector, connected to a 1.5 m AgX Fiber DST series (6.5 mm × 203 mm) probe with a silicon sensor.

Cyclic voltammetry was performed in a LC Technology Solutions Inc. LC-200 glovebox under an N_2 atmosphere using a CH Instruments model 620E potentiostat. Measurements were performed using standard three-electrode cell containing a 1 mm PEEK-encased glassy carbon working electrode, a 3 mm glassy carbon rod (Alfa) as the counter electrode, and a silver wire suspended in electrolyte solution and separated from the analyte solution by a glass frit (CH Instruments 112) as the pseudo-reference electrode in THF with 0.20 M $[Bu_4N][B(C_6F_5)_4]$ for **1** and $[Bu_4N][PF_6]$ for **2** as the supporting electrolyte. The working electrode was polished using 0.05 μm γ-alumina and rinsed with THF before use. Ferrocene was used as an internal reference, and all potentials are reported versus the ferrocenium/ferrocene couple at 0.0 V.

Hydrogen gas generated in the catalytic N_2 reduction reactions was quantified using an Agilent Technologies 7820A GC System. The GC parameters for H_2 quantification on the Agilent 7820A GC System are as follows: Column: Supelco Analytical 60/80 Carboxen 1000, 15ft × 1/8 in × 2.1 mm SS. Inlet temperature: 230 °C; Flow: 30 mL/min; oven temperature and ramp program: initial temperature 35 °C, hold 10 min, 20 °C to 220 °C. hold 10.75 min.; Carrier gas: Ar; Detector: Thermal Conductivity Detector at 250 °C. UltraHigh Purity He gas (99.999%) was used as an internal standard for H_2 quantification. The gas response factors for H_2 and He were determined by obtaining an average from repeated injections (> 20 trials) of 0.20 mL of a calibration gas (an ultrapure, research grade, premixed primary gas standard of H_2 (0.500%), He (0.503%), N_2 (4.980%), with the balance gas of argon) which was purchased from PurityPlus Specialty Gases. With He normalized as 1.0, the H_2 response factor were determined to be 1.01, for this gas quantification method. The gas retention times of He, H_2, N_2 were recorded as ~ 0.9, 1.1 and 5.1 min, respectively using the GC method listed above.

UV-Vis data were recorded using an Ocean Optics Flame-S UV-Vis spectrophotometer. UV-Vis samples were recorded in a cuvette with a 1 cm pathlength.

LIFDI-MS spectra acquired with a GCT Waters Q-TOF Premier (Waters, Manchester, UK) upgraded with a standard LIFDI source (Linden CMS, Weyhe, Germany). Analyte solutions (ca. 0.1-1 mmol/L with 1 μL THF) were prepared in autosampler vials capped with a rubber septum. A silica fused capillary punched through the septa of vials allowing for rinsing of the capillary by means of the inert headspace gas. The capillary was then dipped into sample solution for ca. 3 s wetting the emitter wire, which was heated to 120 mA with a standard Emitter Heating Current (EHC) ramp of 30 mA/min. The subsequent data acquisition was performed at -10 kV at the counter electrode for cation measurements.

Synthesis and Materials

All synthetic procedures were performed under an atmosphere of N_2 using standard Schlenk or glovebox techniques. Unless described otherwise, all reagents were purchased from commercial sources and were used as received. Proteo solvents were sparged and stored under Ultra High Purity (UHP) argon gas before being dried via passage through a CHEMBLY solvent purification system (formerly JC Meyer Solvent Systems) using UHP argon as the working gas and stored under N_2 until use. Deuterated solvents were purchased from Acros Chemical, or Cambridge Isotope Labs, degassed by three freeze-pump-thaw cycles, and stored in an N_2 or Ar filled glovebox over activated molecular sieves. $^{15}N_2$ was purchased from Cambridge Isotope Laboratories. All glassware was heated to 160 °C overnight prior to use. HCl Et_2O, 1,2-diiodoethane and hydrazine dihydrochloride were purchased from ThermoScientific. 4-dimethylaminobenzaldehyde and 1,3,5-trimethoxybenzene were purchased from Acros Chemical. CO gas was purchased from Gas Innovations as C.P. grade (>99.5%). Samarium powder ~40 mesh was purchased from Beantown Chemical. 1,2-bis(dimethylphosphino)ethane and 1,2-bis(diethylphosphino)ethane, were purchased from TCI. 12 M HCl (aq) was purchased from Fisher Chemical. Magnesium powder ~325 mesh was purchased from Alfa Aesar. $CrCl_2(THF)$[1], $SmI_2(THF)_2$[2], *trans*-$[CrCl_2(dmpe)_2]$[3] (**2-Cl**), *trans*-$[Cr(N_2)_2(dmpe)_2]$[4] (**2**), and *trans*-$[CrCl_2(depe)_2]$[5] (**1-Cl**) were prepared following published literature procedures.

Synthesis of *trans*-$[Cr(N_2)_2(depe)_2]$ (1)

Mg(s) (0.116 g, 4.78 mmol, 325 mesh) was added to a stirring solution of $CrCl_2(depe)_2$ (0.112 g, 0.21 mmol) in THF (10 mL), and stirred for 24 h. The deep red solution was dried under reduced pressure and extracted with 5 mL × 3 of Et_2O, filtered through a pad of Celite to remove excess Mg and $MgCl_2$ solids. The dark red solution was dried under reduced pressure and extracted with 5 mL × 3 of pentane and filtered through Celite. The pentane solution was reduced in volume ca. 2 mL and recrystallized by slow evaporation of pentane at -30 °C to afford red blocks or long red needles. Yield: 76 mg (0.14 mmol, 70% yield). ^{1}H NMR (500 MHz, C_6D_6): δ 1.02 (q, 24H, CH_3), 1.42 (d, 8H, PCH_2CH_2P), 1.81 (m, 8H, PCH_2CH$_3$), 1.90 (m, 8H, PCH_2CH$_3$). ^{13}C{^{1}H} NMR (500 MHz, C_6D_6): δ 8.87 (s, PCH$_2$*C*H$_3$), 20.17 (s, P*C*H$_2$*C*H$_2$P), 22.44 (m, P*C*H$_2$CH$_3$). ^{31}P{^{1}H} NMR (500 MHz, C_6D_6): δ 80.07 (s, 4P); IR (THF): ν_{NN} cm^{-1} = 1906; (PhF): ν_{NN} cm^{-1} = 1901. Anal. Calcd. for $C_{20}H_{48}P_4N_4Cr$: C, 46.15%; H, 9.29%; N, 10.76%. Found: C, 45.79%; H, 9.30%; N, 7.68%. Low nitrogen content likely due to N_2 ligand loss during handling and sample analysis. LIFDI-MS: calcd. for $CrP_4C_{20}H_{48}N_4$ $(M)^+$ 520.223 *m/z*, found $(M)^+$ 520.215 *m/z* (100%).

Preparative scale synthesis of *cis*-$[Cr(CO)_2(depe)_2]$ (*cis*-1-CO)

In an N_2 atmosphere glovebox, *trans*-$[Cr(N_2)_2(depe)_2]$ (0.052 g, 0.10 mmol) was added to a scintillation vial and dissolved in ~10 mL THF and sealed with a septum. Outside of the glovebox CO gas was bubbled through the solution for 20 s while stirring. The reaction was stirred for 24 h and a color change from red to yellow was observed. The reaction was dried under vacuum and brought into the glovebox. The dried yellow tacky solids were extracted with Et_2O and filtered through a pad of Celite and syringe filter. The yellow solute was dried under vacuum and subsequently dissolved in pentane, filtered again through a pad of Celite and a syringe filter. Attempts at crystallization via slow evaporation and solvent layering afforded a tacky yellow solid due to minor quantities of free depe liberated in the reaction hampering efforts to obtain

analytically pure material and single crystals for x-ray diffraction. ^{1}H NMR (500 MHz, C_7D_8): δ 0.82 (q, PCH_2CH_3), 0.90 (m, PCH_2CH_3), 1.02 (m, PCH_2CH_3), 1.11 (q, PCH_2CH_3), 1.29 (m, PCH_2CH_2P and PCH_2CH_3), 1.38 (m, PCH_2CH_2P and PCH_2CH_3), 1.53 (m, PCH_2CH_3), 1.69 (m, PCH_2CH_3), 1.85 (m, PCH_2CH_3), 2.02 (m, PCH_2CH_3). $^{31}P\{^{1}H\}$ NMR (500 MHz, C_6D_6,): δ 86.6 (m), 62.9 (m); IR (pentane): ν_{CO} cm^{-1} = 1843,1784; (Et_2O) ν_{CO} cm^{-1} = 1835, 1776. LIFDI-MS: calcd. for $CrP_4C_{22}H_{48}O_2$ $(M)^+$ 520.201 *m/z*, found $(M)^+$ 520.190 *m/z* (100%).

Experimental Protocol for Catalytic N_2 reduction

A two neck 25 mL round bottom reaction flask and a Teflon valve were acid cleaned with HCl, oven dried and brought into the glovebox. From a stock solution of the Cr catalyst in THF, 0.6 μmol of catalyst was dispensed into the reaction vessel. $SmI_2(THF)_2$ was weighed as a solid and added to the reaction vessel. 15 mL of THF was added, and the reaction was stirred to combine both the catalyst and reductant resulting in a dark blue solution. Finally, depending on the proton source used the entire sealed reaction vessel was brought outside of the glovebox to add degassed H_2O via a degassed syringe and needle, or a known amount of ethylene glycol was added inside the glovebox as a solution dissolved in THF. The reaction was sealed and stirred for the specified time. (Note: upon addition of large amounts of proton source the reaction will immediately change from dark blue to dark red). Once the reaction changed to an off-white or yellow color the product analysis protocols were initiated. All reactions performed with ethylene glycol after stirring for 48 h were blue upon analysis. Entries 18, 19, and 20 from Table S1 were stirred for 100 h, 120 h, and 141 h, respectively, these reactions were white upon analysis. All the catalytic reactions performed with H_2O from 3 h to 48 h were white upon analysis. For catalysis performed using an $^{15}N_2$ atmosphere, the same protocol was followed except prior to the addition of the proton source the reaction solution was degassed, frozen in liquid nitrogen and the headspace backfilled with 1 atm of $^{15}N_2$. The product quantification protocols described below were performed in the following order: 1) N_2H_4, 2) H_2, 3) NH_3.

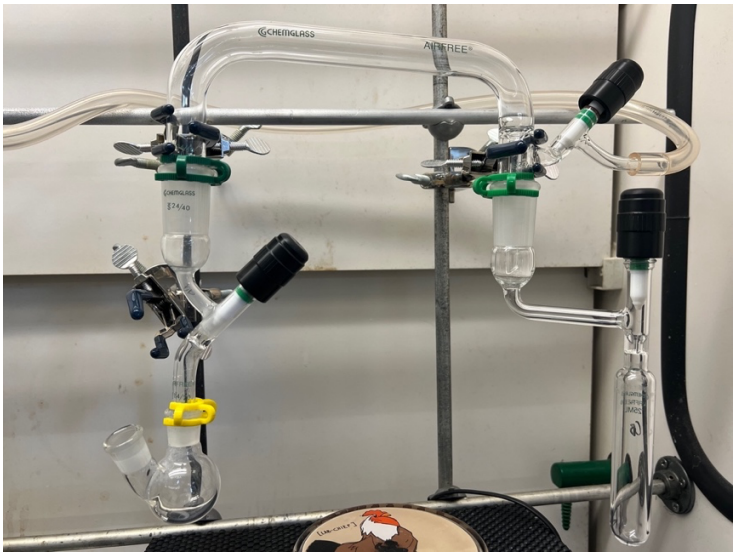

Figure S1. Assembled apparatus used for NH_3 quantification from catalytic N_2 reduction experiments. Reaction flask (left) connected via Teflon-valved adapter to transfer manifold (above) connected to a receiving flask (right) with a Teflon valve, transfer manifold is connected to N_2 and vacuum.

Hydrazine Quantification Protocol

Hydrazine was quantified following the method described by Watt and Chrisp.[6] 0.4 g of 4-dimethylaminobenzaldehyde was dissolved in 20 mL of ethanol and 2 mL of 12 M HCl was added to form a green indicator solution. This solution was stirred for at least 10 min before use. A quartz cuvette (path length of 1.0 cm) was filled with the indicator solution to reference as the background in the UV-Vis. 10 mL of the indicator solution was placed into a 25 mL volumetric flask. A using a degassed syringe and needle, 1 mL of reaction solution was removed and quickly added to the volumetric flask. The flask was then filled to the 25 mL line with 1 M HCl. This solution was then stirred for 10 min, then a quartz cuvette was filled with the solution and a UV-Vis spectrum was recorded. The absorbance value at 458 nm was measured. A previously prepared calibration curve (**Figure S2**) was used to determine the amount of hydrazine present in the sample.

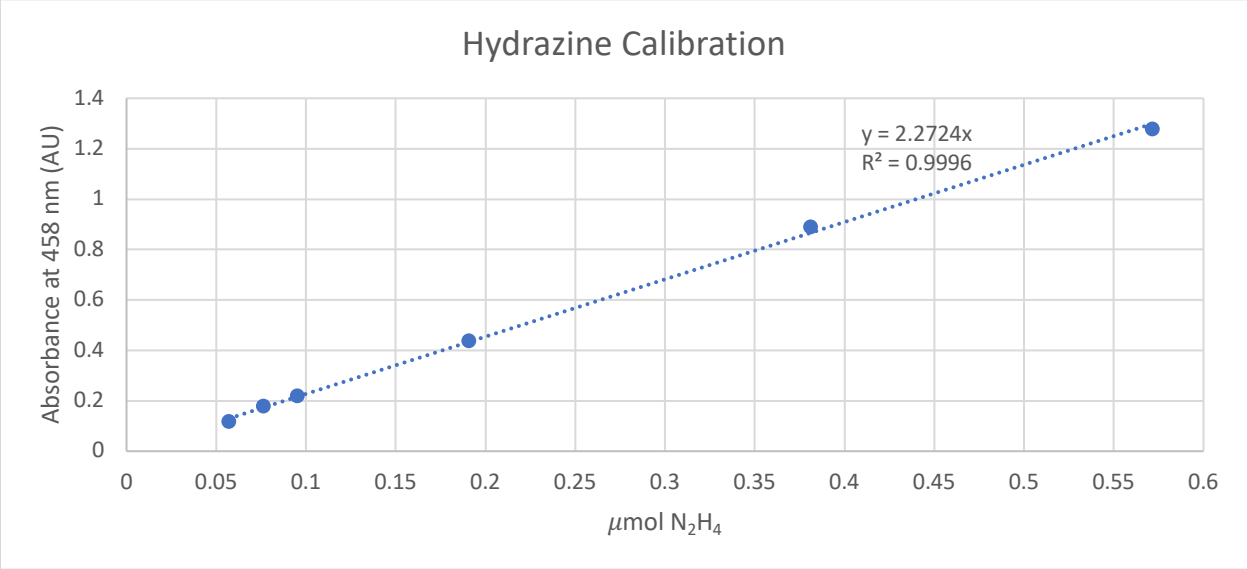

Figure S2. Hydrazine calibration curve using 4-dimethylaminobenzaldehyde colorimetric protocol for use in quantification of hydrazine.

Hydrogen Quantification Protocol

The GC method was loaded, and an injection of the calibration gas was run prior to use. A gas tight syringe was purged with argon, filled with 0.25 µL helium as an internal standard and injected into the head space of the reaction vessel. The reaction was stirred for 10 min. The reaction solution was frozen with liquid nitrogen to prevent loss of NH_3 in the head space. The gas tight syringe was again purged with argon and 0.25 µL sample of the head space was removed and injected into the GC. The amount of hydrogen produced was determined from the peak area of He and H_2.

Ammonia Quantification Protocol

Ammonia was quantified following previous literature procedures.[4, 7] Once the H_2 and N_2H_4 quantification procedures were completed the reaction flask was submerged in liquid nitrogen to freeze the reaction solution. 1 M HCl etherate was added to a receiving flask and both flasks are connected to a transfer manifold (**Figure S1**). The receiving flask was also submerged in liquid nitrogen. Once both solutions were frozen, the entire apparatus was opened to vacuum for 5 min. The reaction flask was then sealed while the receiving flask remains open. A 40% w/w solution of KOH was added to the reaction flask. The reaction flask was warmed to room temperature. Once warmed, the manifold was placed under static vacuum. The receiving flask submerged in liquid nitrogen remained open to the manifold. The reaction flask was then slowly opened to the manifold and the volatiles were vacuum transferred to the receiving flask. The receiving flask was closed, warmed to room temperature, and stirred for ~10 min. The volatiles were removed from the receiving flask under reduced pressure leaving behind a white residue that was dissolved in a 0.5 mL solution of DMSO-d_6 containing the internal standard of 1,3,5-trimethoxybenzene.

Preparation of $\mathbf{1^{15N}}$ and $\mathbf{2^{15N}}$ ($^{14}N_2/^{15}N_2$ exchange experiments)
In a nitrogen atmosphere glovebox, a a Teflon valved NMR tube is charged with ~10 mg of **1** or **2** in ~1 mL of THF-d_8 or benzene-d_6. The NMR tube was brought outside of the glovebox, frozen in liquid nitrogen, and degassed by performing three, freeze-pump-thaw cycles. After the last cycle the frozen solution was placed under vacuum, attached to a custom-made low-volume manifold connected to a digital vacuum gauge. The manifold was connected to a 1 L lecture bottle of $^{15}N_2$. The NMR tube was then placed under 1 atm of $^{15}N_2$ and warmed to room temperature. The NMR tube was placed on a NMR tube rotator/spinner with a rate of 5 rpm to mix the gas and liquid phase. The reaction was monitored by ^{15}N NMR spectroscopy, with the full ^{15}N NMR spectrum collected after mixing for 24 h.

Attempted reduction of 1-Cl with SmI_2THF to generate 1.

SmI_2THF (0.079 g, 0.14 mmol, 5 equiv.) was added as a solid to a stirring solution of **1-Cl** (0.0154 g, 0.03 mmol, 1 equiv.) in ~5 mL of THF. The reaction was stirred vigorously for 24 h. The solvent was removed under reduced pressure leaving behind blue solids. The solid was extracted with ~5 mL of pentane, filtered through Celite. The pentane solution was reduced in volume to ~2 mL and stored at -30 °C. The solid residue was dissolved in THF an analyzed by $^{31}P\{^1H\}$ NMR spectroscopy. No ^{31}P signals were observed. A diagnostic singlet for **1** appears at 80 ppm in the ^{31}P NMR spectrum in THF.

Attempted reduction of 2-Cl with SmI_2THF to generate 2.

SmI_2THF (0.110 g, 0.20 mmol, 5 equiv.) was added as a solid to a stirring solution of **2-Cl** (0.017 g, 0.040 mmol, 1 equiv.), in ~5 mL of THF. The reaction was stirred vigorously for 24 h. The solvent was removed under reduced pressure leaving blue solids. The products were then extracted with ~5 mL of pentane and the solution filtered through Celite. The yellow pentane solution was reduced in volume to ~2 mL and stored at -30 °C upon which time dark orange/red crystals formed. The remaining pentane solution was decanted off. The dark orange crystals were dissolved THF and examined by $^{31}P\{^1H\}$ NMR spectroscopy. No ^{31}P signals were observed. A diagnostic singlet

for **2** appears at 68 ppm in the ^{31}P NMR spectrum in THF. The dark orange crystals were identified as trans-[$CrI_2(dmpe)_2$] indicating halide ligand exchange had occurred in the reaction.

Reaction of 1-Cl with 2 equiv SmI_2THF in the presence of ethylene glycol

1-Cl (11.7 mg, 0.022 mmol, 1 equiv.) and SmI_2THF (24 mg, 0.044 mmol, 2 equiv.) were dissolved in ~1 mL of THF and added to a Teflon-valved NMR tube as a blue suspension. Ethylene glycol (2.7 mg, 0.044 mmol, 2 equiv.) in 150 μL of THF was the added to the NMR tube and the tube was immediately sealed. The solution immediately changed from a blue suspension to a light green solution and concomitant formation of a dark brown solid. The reaction was immediately monitored by ^{31}P NMR spectroscopy. No ^{31}P NMR signals were observed. We conclude that either the reduction potential of SmI_2THF and ethylene glycol is insufficient to reduce Cr(II) to Cr(0), or using these reaction conditions **1-Cl**, **1**, or a species formed en route to **1** is unstable and the coordination complex decomposes.

Reaction of 2-Cl with 2 equiv SmI_2THF in the presence of ethylene glycol

2-Cl (12.6 mg, 0.03 mmol, 1 equiv.) and SmI_2THF (33 mg, 0.06 mmol, 2 equiv.) were dissolved in ~1 mL of THF and added to a Teflon-valved NMR tube as a blue suspension. Ethylene glycol (3.7 mg, 0.06 mmol, 2 equiv.) in 150 μL of THF was the added to the NMR tube and the tube was immediately sealed. Upon the addition of ethylene glycol the solution immediately changed from dark blue to yellow and the appearance of a white solid. The $^{31}P\{^1H\}$ NMR spectrum contained a diagnostic singlet at 67.9 ppm corresponding to the formation of **2**.

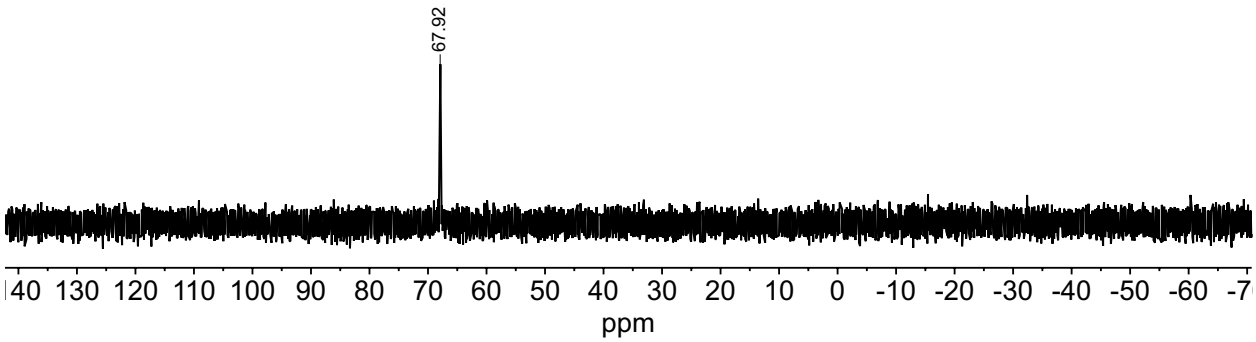

Figure S3. $^{31}P\{^1H\}$ NMR spectrum of the reaction of **2-Cl** with 2 equiv SmI_2THF and 2 equiv ethylene glycol in recorded in THF immediately after mixing showing formation of **2**.

Catalytic Reaction of 2 with added free-dmpe

Catalysis was performed as reported, with a modification of the standard procedure where free-dmpe was added at the same time as the ethylene glycol. Free-dmpe ligand (0.0187 g, 0.124 mmol, 519 equiv.) was mixed with THF and the solution was added to the vial containing the ethylene glycol and the resulting mixture was added to the reaction flask containing the catalyst and SmI_2.

NMR spectral data, Infrared data, cyclic voltammetry and LIFDI-MS results

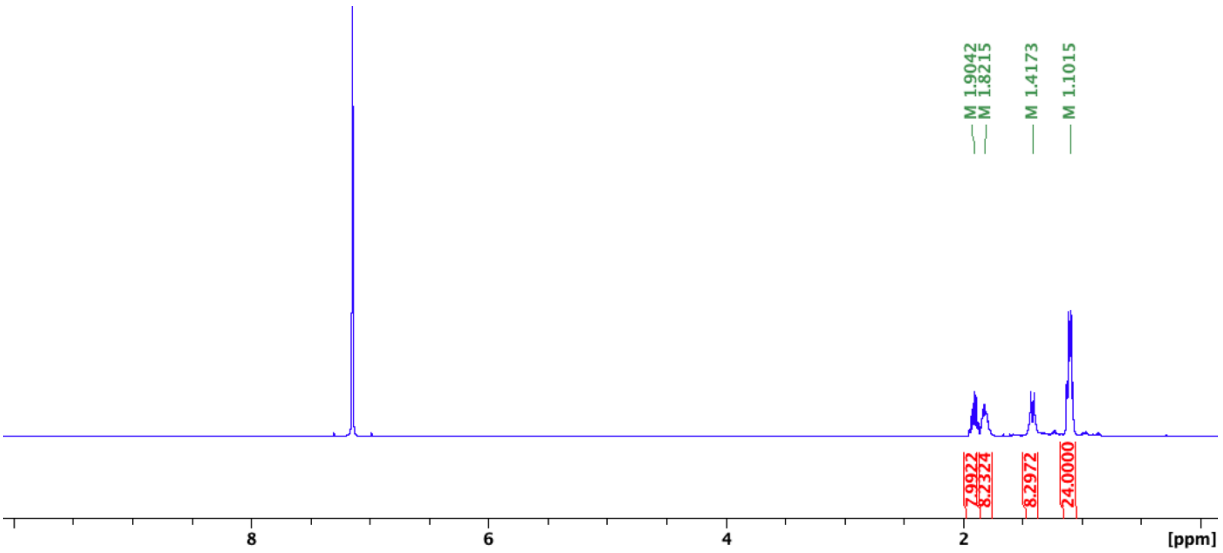

Figure S4. ^{1}H NMR spectrum of *trans*-[$Cr(N_2)_2(depe)_2$] (**1**) in benzene-d_6.

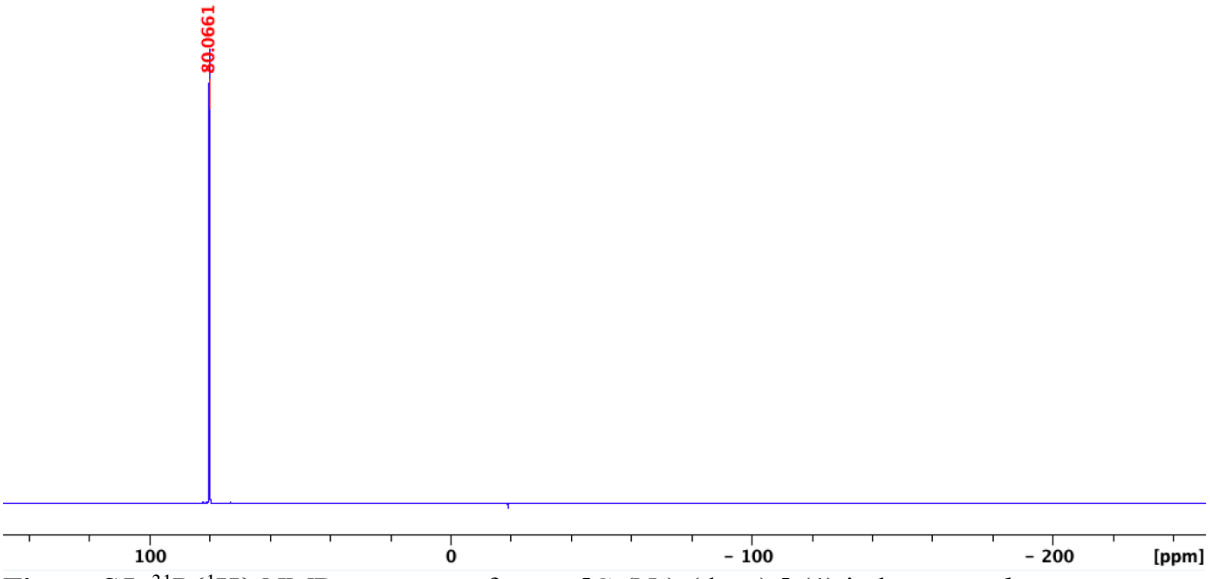

Figure S5. $^{31}P\{^{1}H\}$ NMR spectrum of *trans*-[$Cr(N_2)_2(depe)_2$] (**1**) in benzene-d_6.

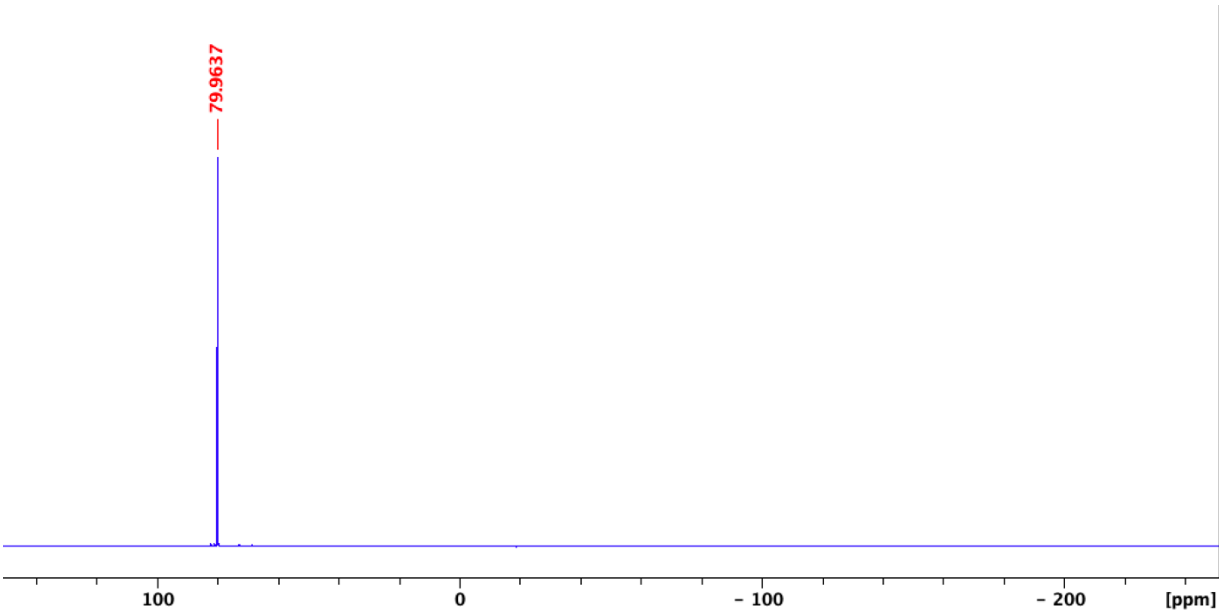

Figure S6. $^{31}P\{^{1}H\}$ NMR spectrum of *trans*-$[Cr(N_2)_2(depe)_2]$ (**1**) in THF-d_8.

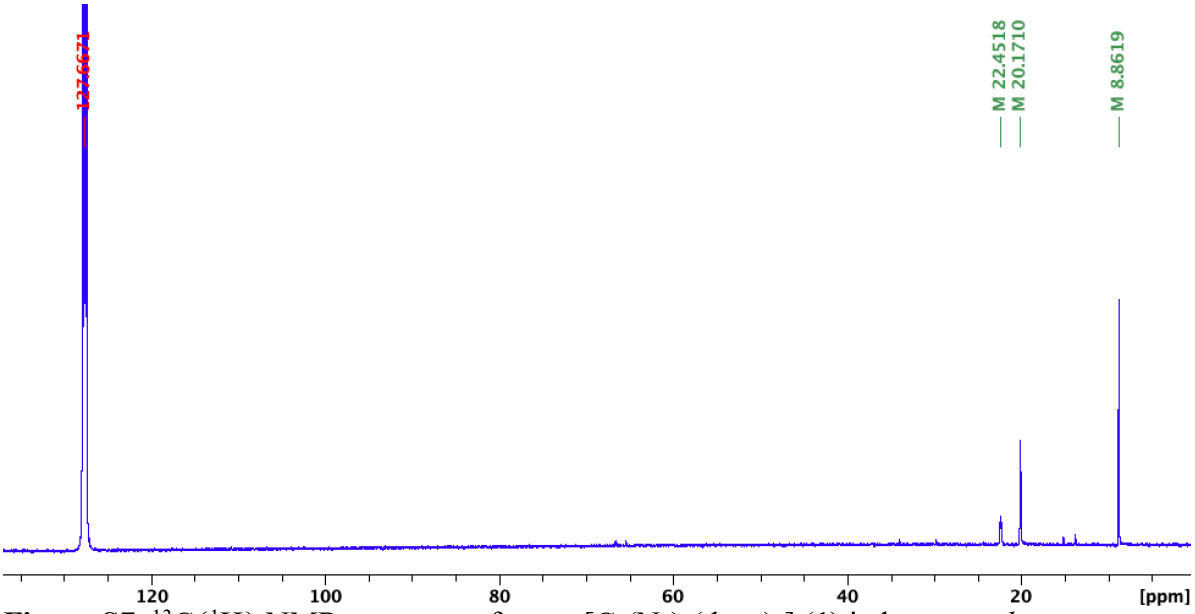

Figure S7. $^{13}C\{^{1}H\}$ NMR spectrum of *trans*-$[Cr(N_2)_2(depe)_2]$ (**1**) in benzene-d_6

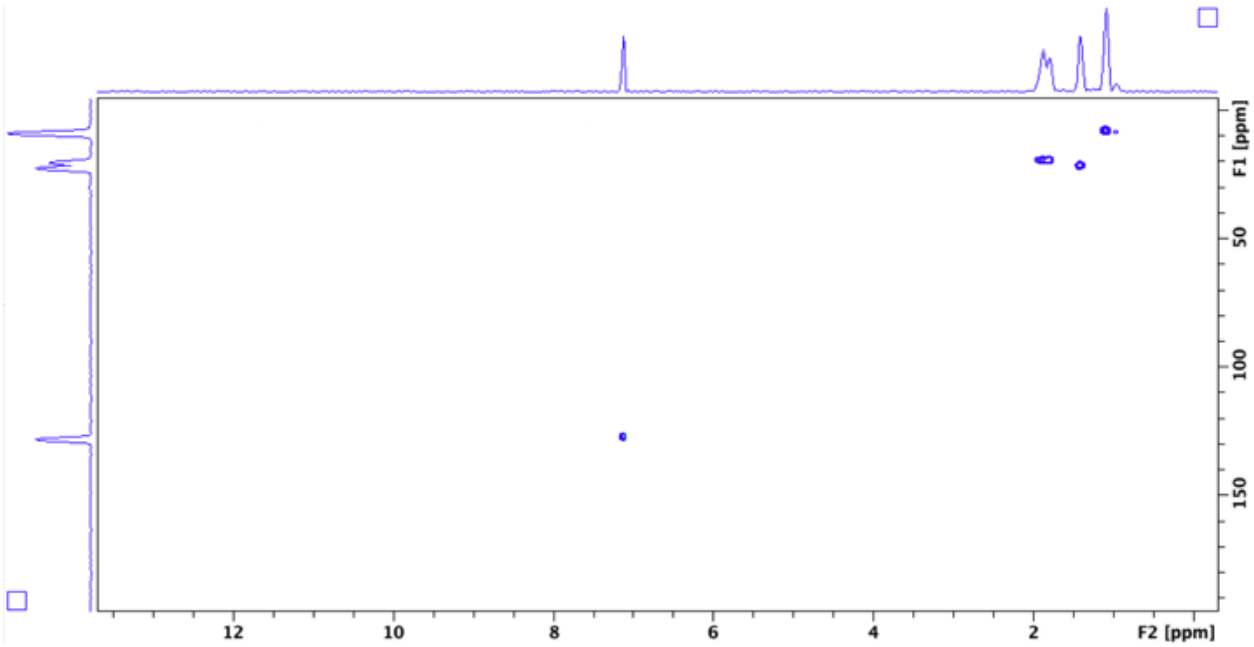

Figure S8. HSQC ^{1}H ^{13}C NMR spectrum of *trans*-[$Cr(N_2)_2(depe)_2$] (**1**) in benzene-d_6.

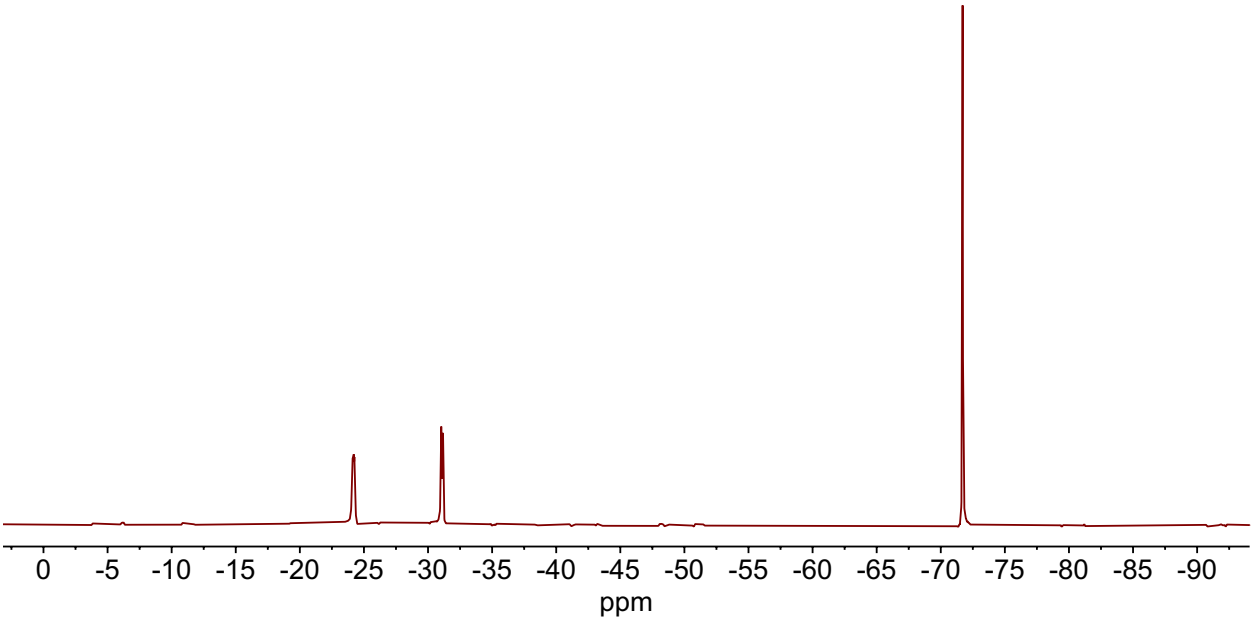

Figure S9. $^{15}N\{^{1}H\}$ NMR spectrum of *trans*-[$Cr(N_2)_2(depe)_2$] (**1**) in THF-d_8.

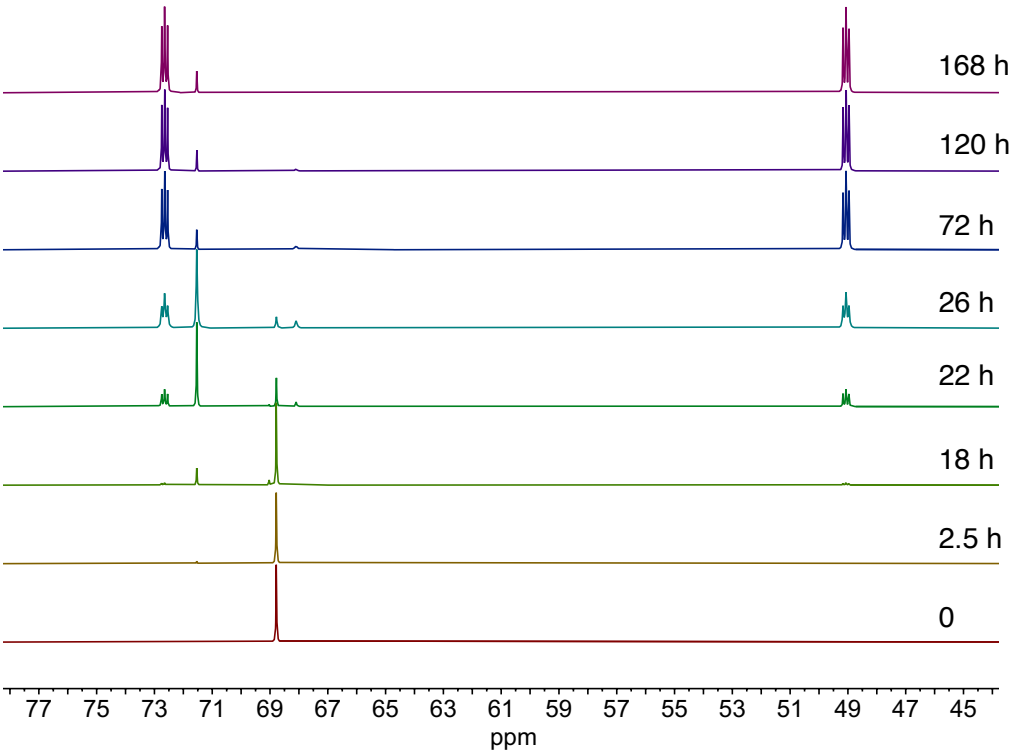

Figure S10. $^{31}P\{^{1}H\}$ NMR spectra recorded in THF-d_8 showing the conversion of **2** to ***cis*-2-CO** from t = 0 h to 168 h. **2**: δ 68.8 (s), *trans*-$[Cr(CO)_2(dmpe)_2]$ ***trans*-2-CO**: δ 71.5 (s), *cis*-$[Cr(CO)_2(dmpe)_2]$: δ 72.65 (m) and δ 49.0 (m), free dmpe at -48.6 ppm not shown, see **Figure S10** for expanded plot.

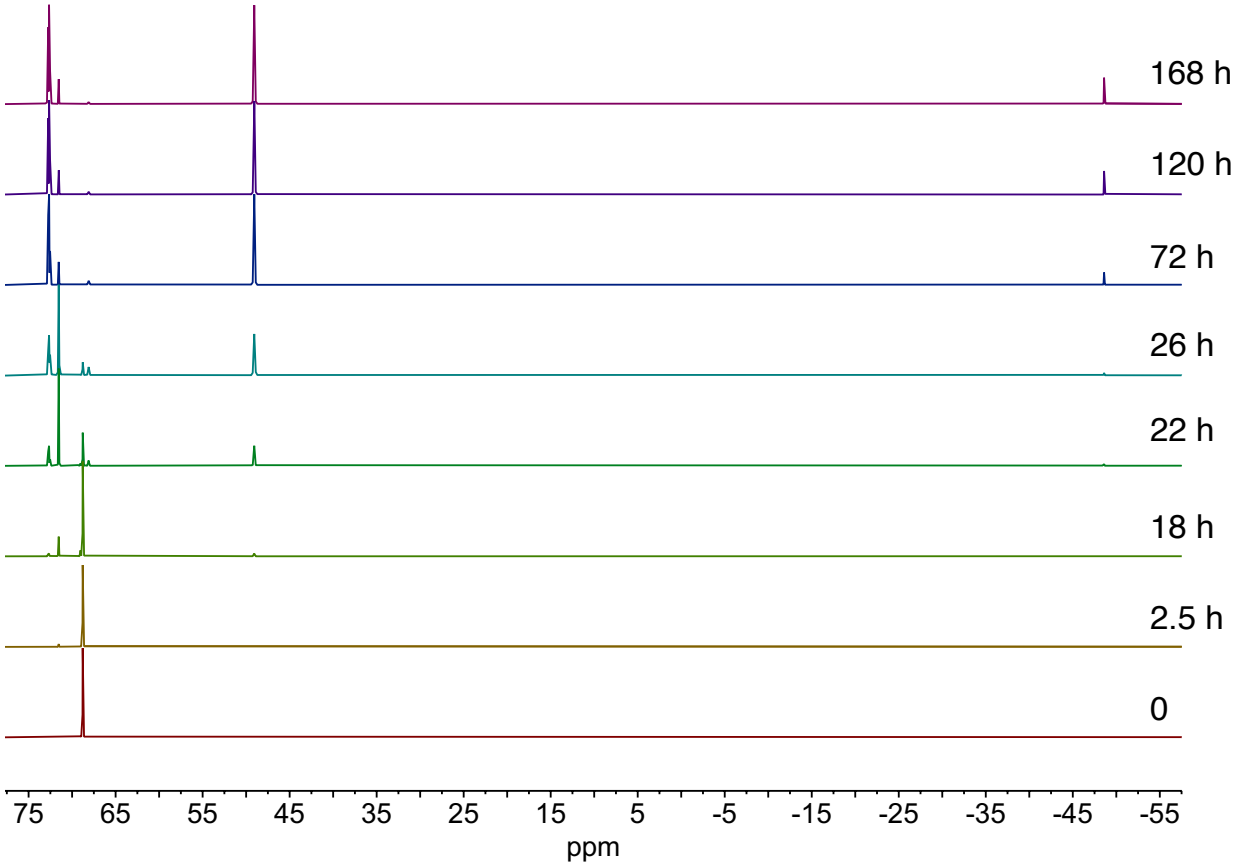

Figure S11. $^{31}P\{^{1}H\}$ NMR spectra recorded in THF-d_8 showing the conversion of **2** to ***cis*-2-CO** from t = 0 h to t = 168 h. Expanded scale to include free dmpe. **2**: δ 68.8 (s), *trans*-$[Cr(CO)_2(dmpe)_2]$: δ 71.5 (s), *cis*-$[Cr(CO)_2(dmpe)_2]$: δ 72.65 (m) and δ 49.0 (m), free dmpe: δ −48.6 (s).

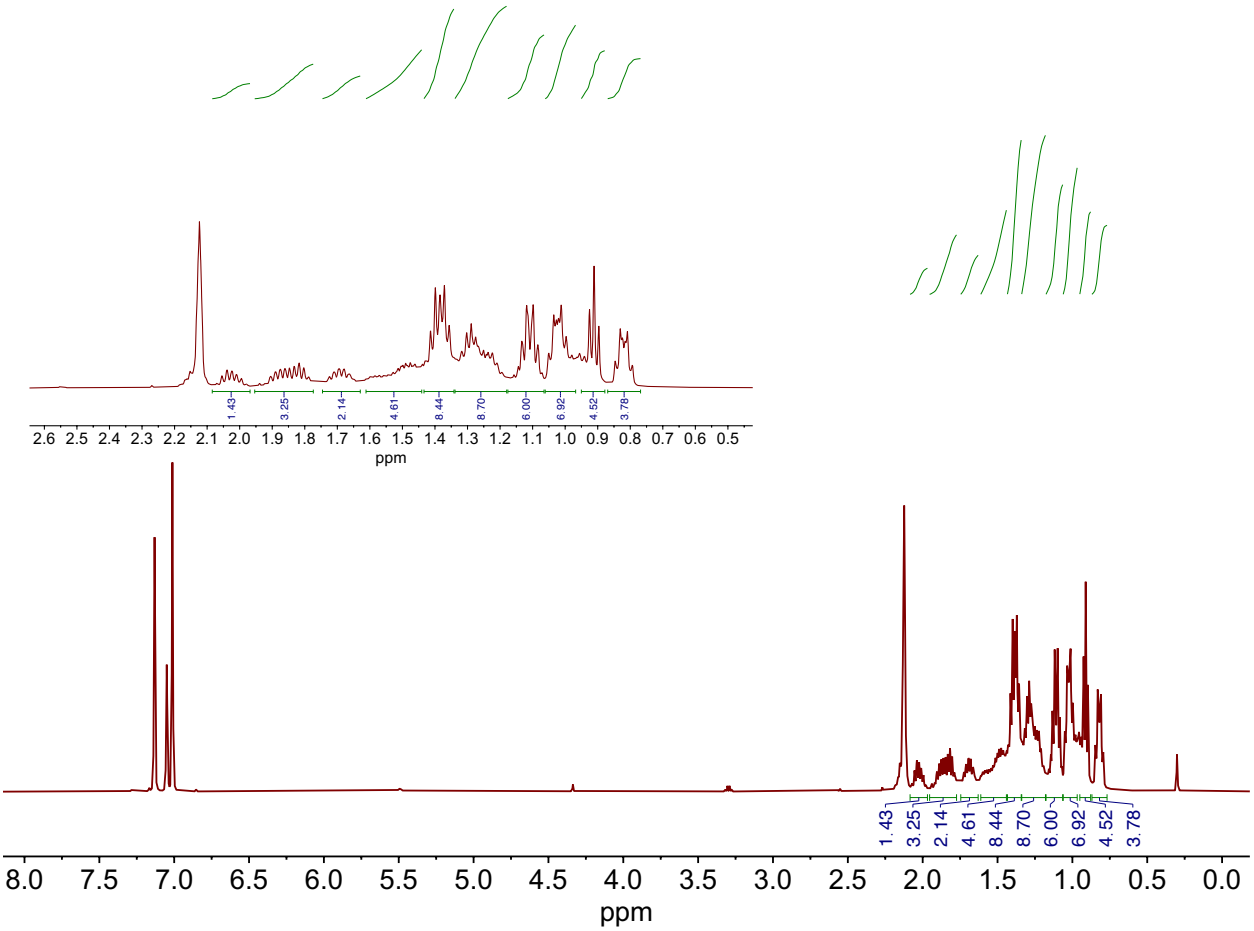

Figure S12. ^{1}H NMR spectrum of *cis*-[Cr(CO)$_2$(depe)$_2$] ***cis*-1-CO** in toluene-d_8.

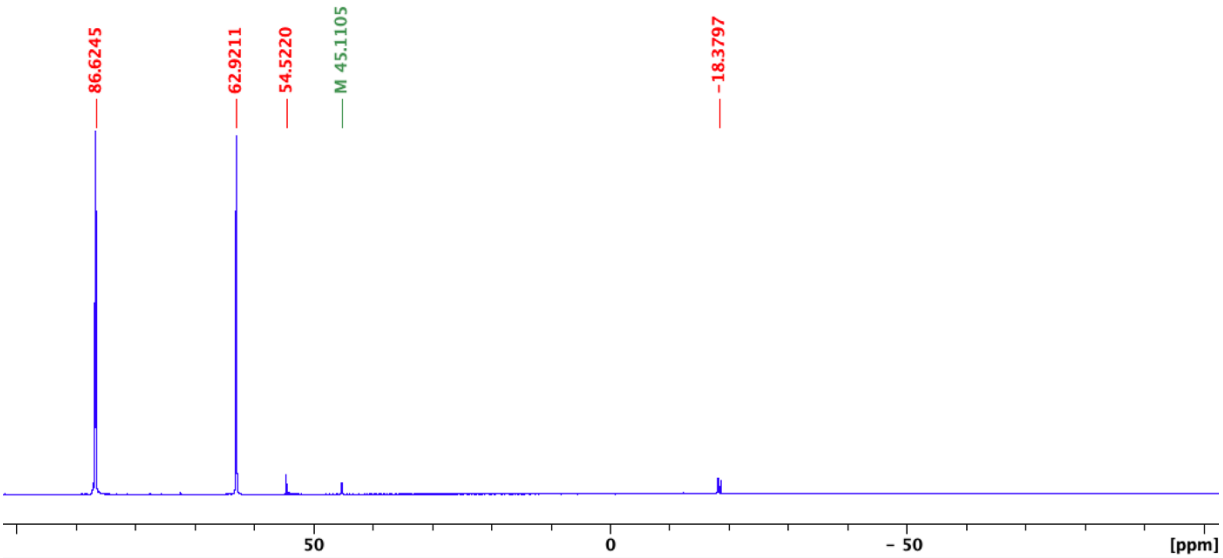

Figure S13. ^{31}P{^{1}H} NMR spectrum of *cis*-[Cr(CO)$_2$(depe)$_2$] ***cis*-1-CO** in THF.

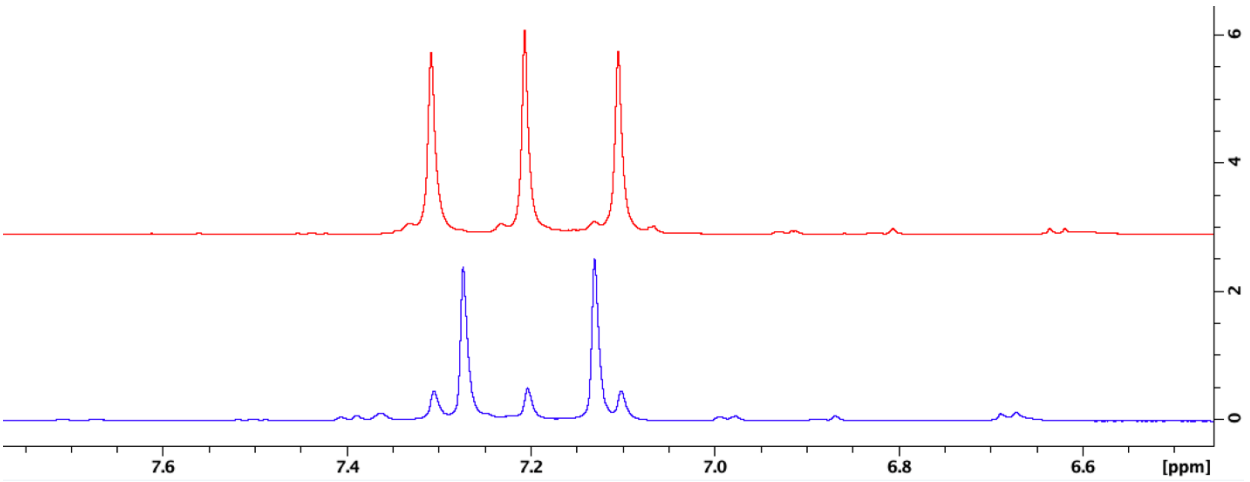

Figure S14. ^{1}H NMR spectra recorded in DMSO-d_6 of $^{14}NH_4Cl$ (red) and $^{15}NH_4Cl$ (blue) from NH_3 quantification protocol. The blue trace represents the $^{15}NH_4Cl$ generated in the catalytic dinitrogen reduction experiment performed under an atmosphere of $^{15}N_2$ using *trans*-[Cr(N_2)$_2$(dmpe)$_2$] (**2**$^{\mathbf{14N}}$) as the precatalyst.

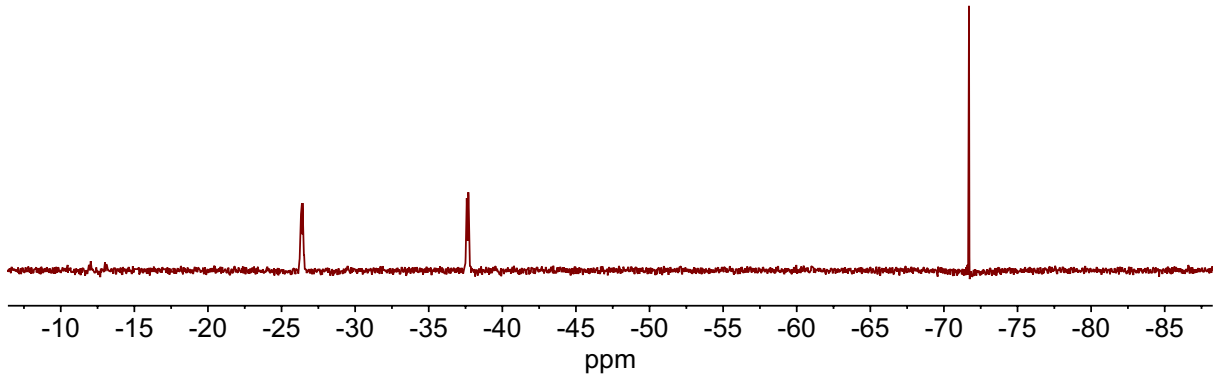

Figure S15. $^{15}N\{^{1}H\}$ NMR spectrum of *trans*-[Cr(N_2)$_2$(dmpe)$_2$] (**2**) in THF-d_8.

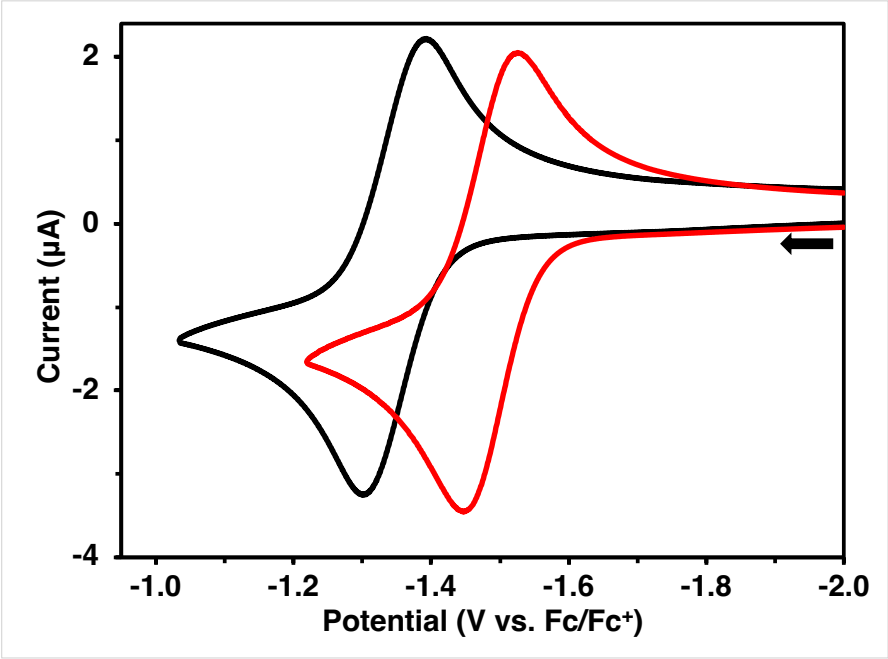

Figure S16. Cyclic voltammograms of **1** and **2** recorded in THF showing the $Cr^{I/0}$ waves.

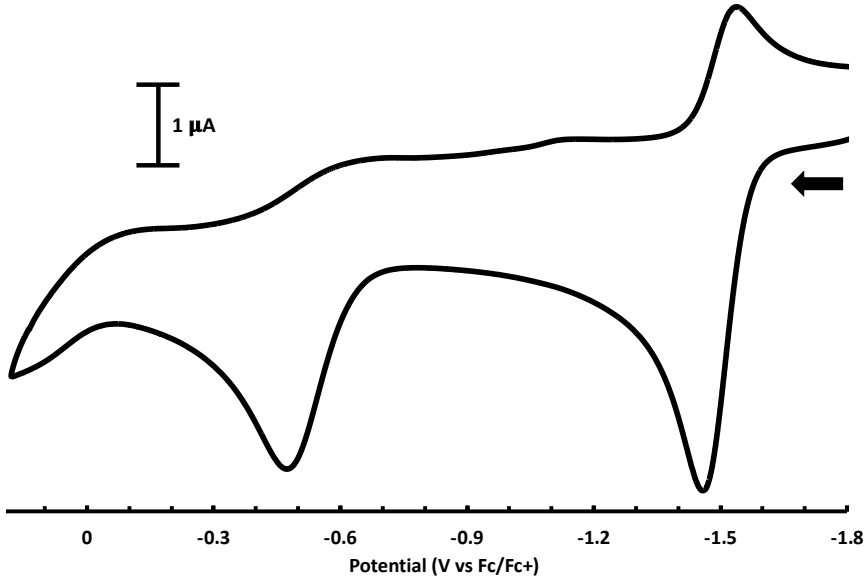

Figure S17. Cyclic voltammogram of **1** recorded in THF at υ = 0.10 V s^{-1}. Conditions: 0.2 M $[Bu_4N][B(C_6F_5)_4]$ solution, glassy carbon working electrode.

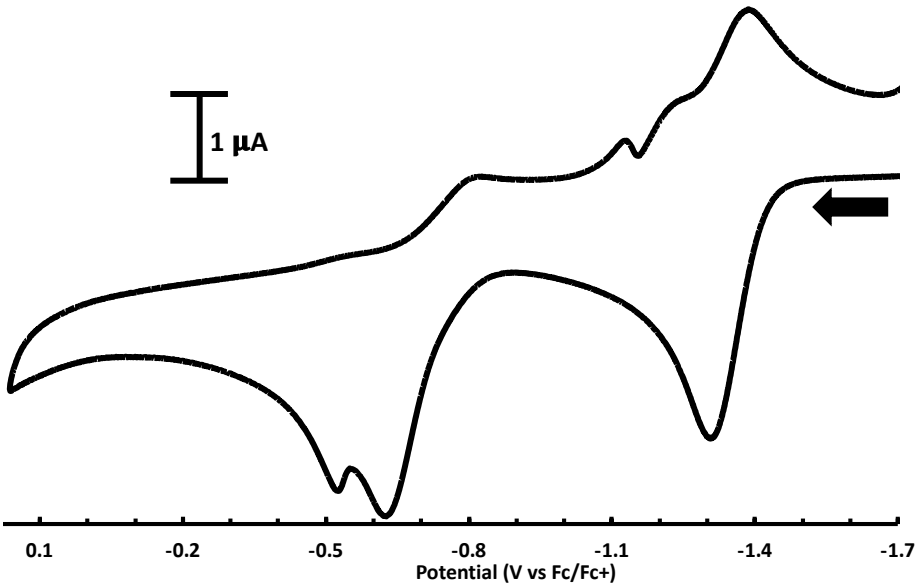

Figure S18. Cyclic voltammogram of **2** recorded in THF at $\upsilon = 0.10$ V s^{-1}. Conditions: 0.2 M $[Bu_4N][PF_6]$ solution, glassy carbon working electrode.

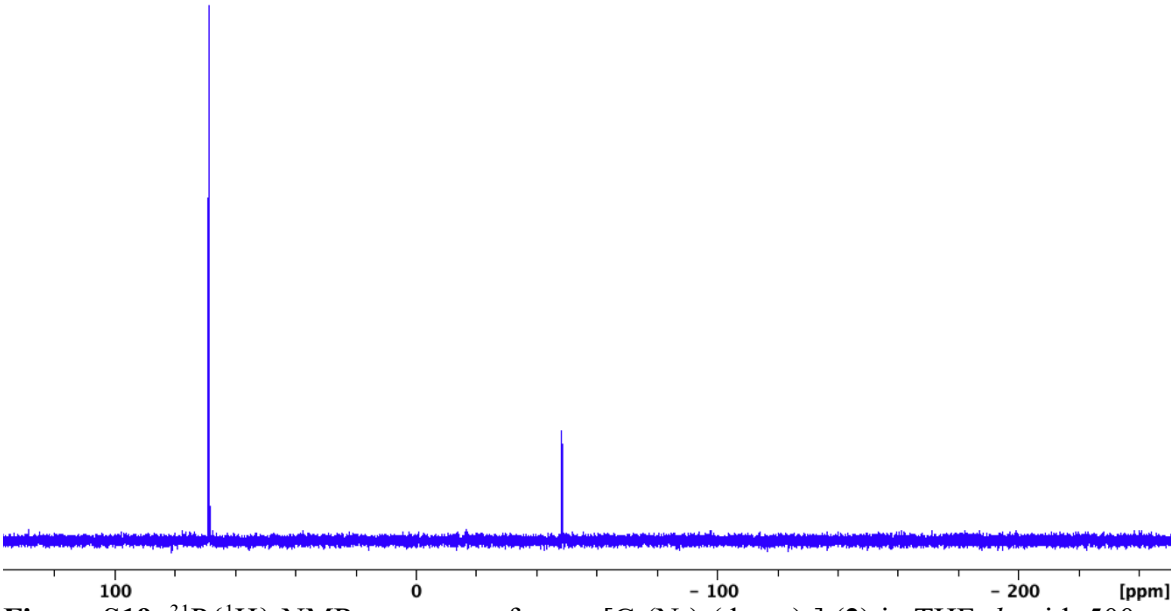

Figure S19. $^{31}P\{^{1}H\}$ NMR spectrum of *trans*-$[Cr(N_2)_2(dmpe)_2]$ (**2**) in THF-d_8 with 500 equiv of ethylene glycol after 2 h, free dmpe at −48.6.

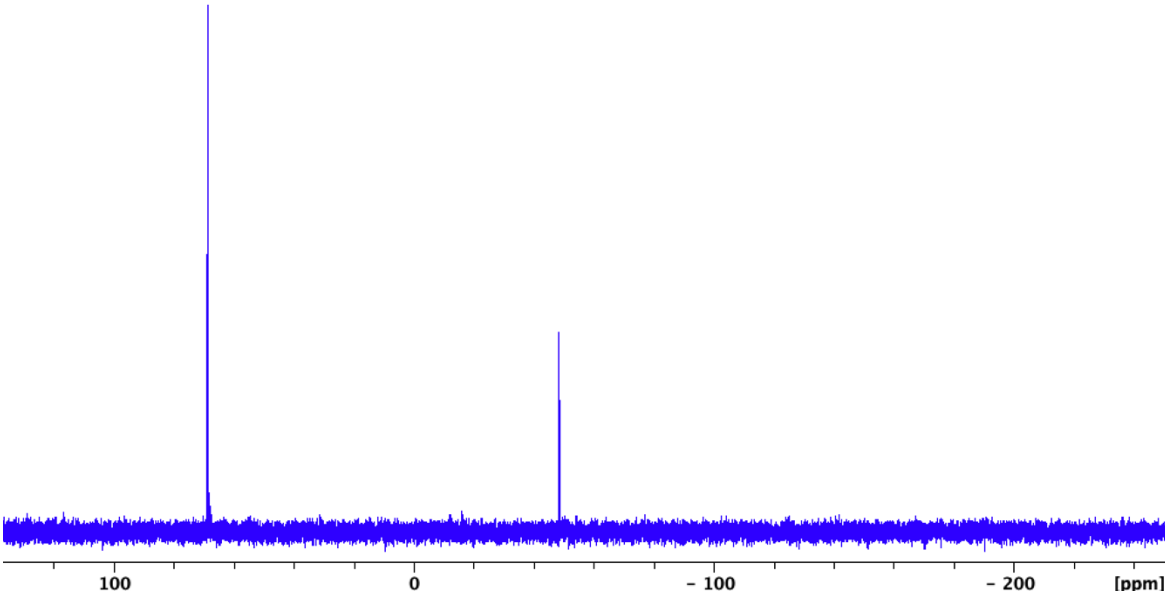

Figure S20. ^{31}P NMR spectrum of *trans*-$[Cr(N_2)_2(dmpe)_2]$ (**2**) recorded in THF-d_8 with 500 equiv of H_2O after 2 h, free dmpe at −48.6.

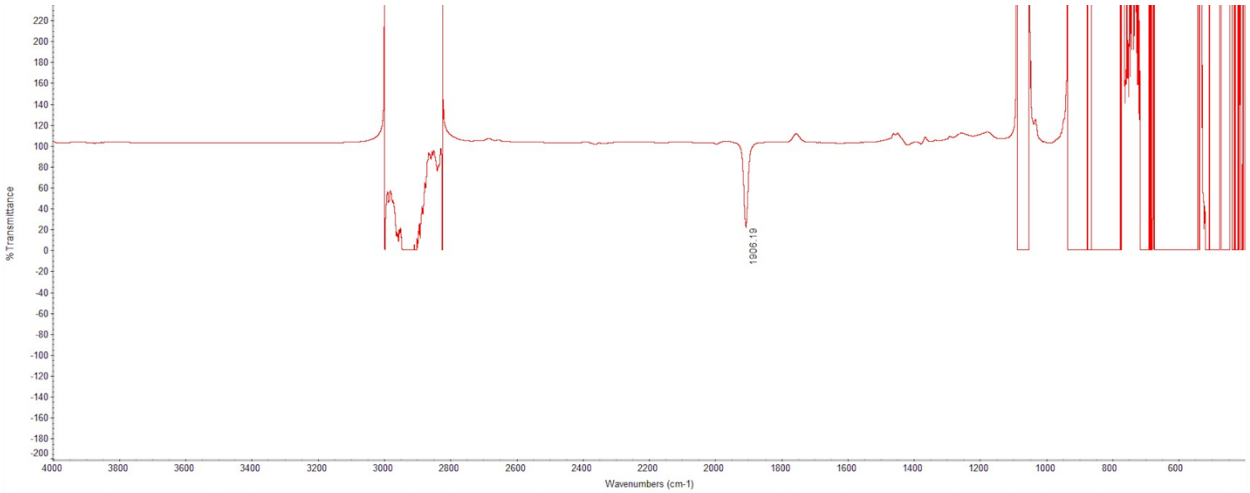

Figure S21. Infrared spectrum of *trans*-[Cr(N$_2$)$_2$(depe)$_2$] (**1**) recorded in THF.

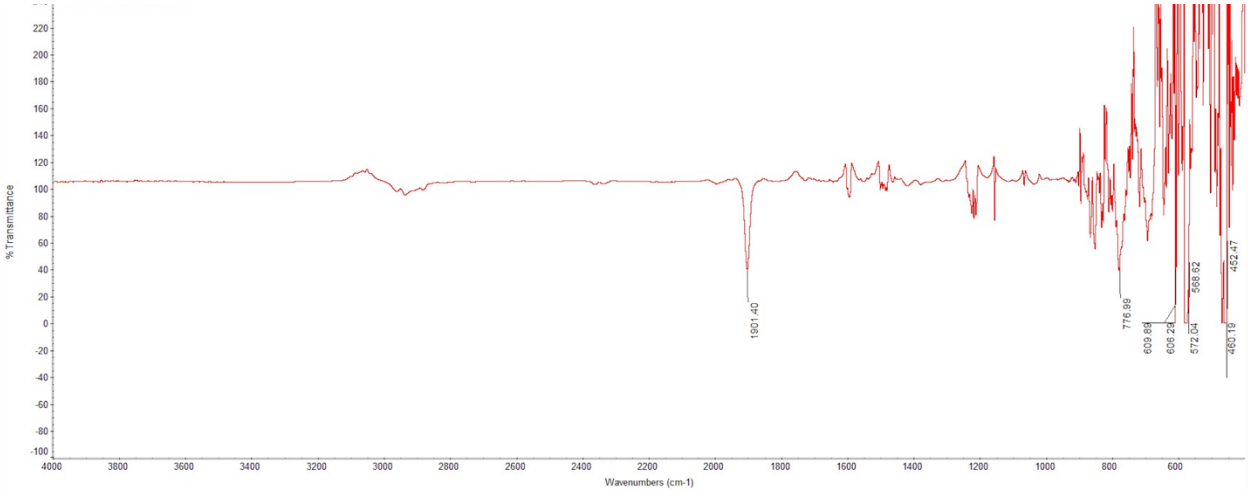

Figure S22. Infrared spectrum of *trans*-[Cr(N$_2$)$_2$(depe)$_2$] (**1**) recorded in fluorobenzene.

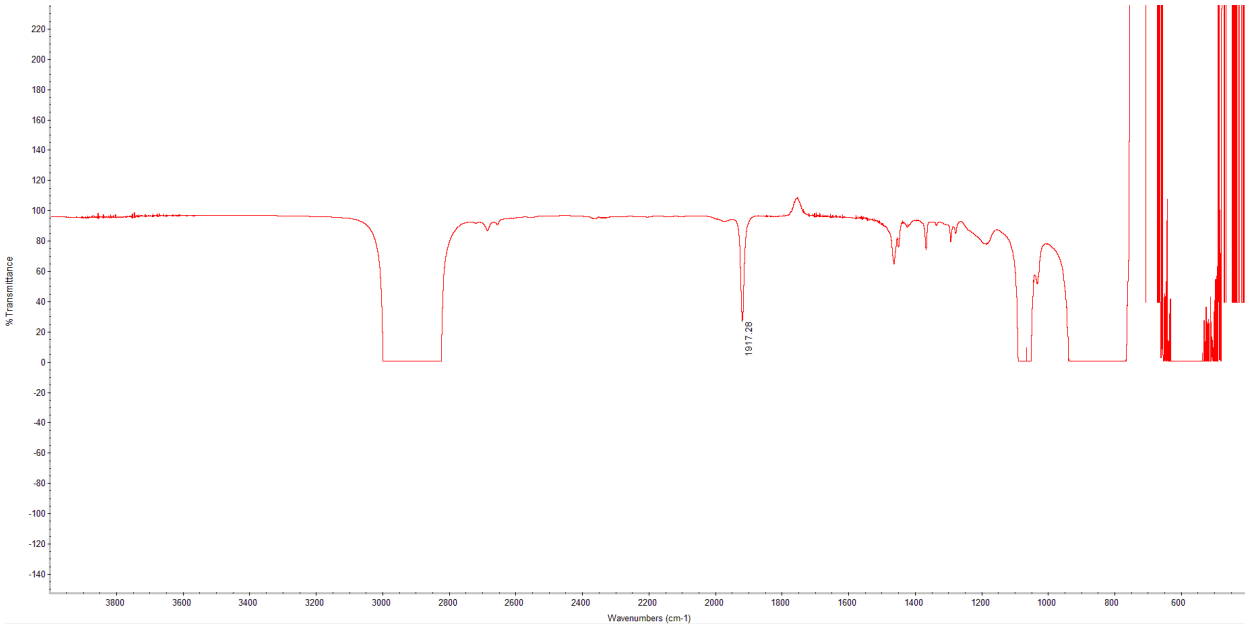

Figure S23. Infrared spectrum of *trans*-[$Cr(N_2)_2(dmpe)_2$] (**2**) recorded in THF.

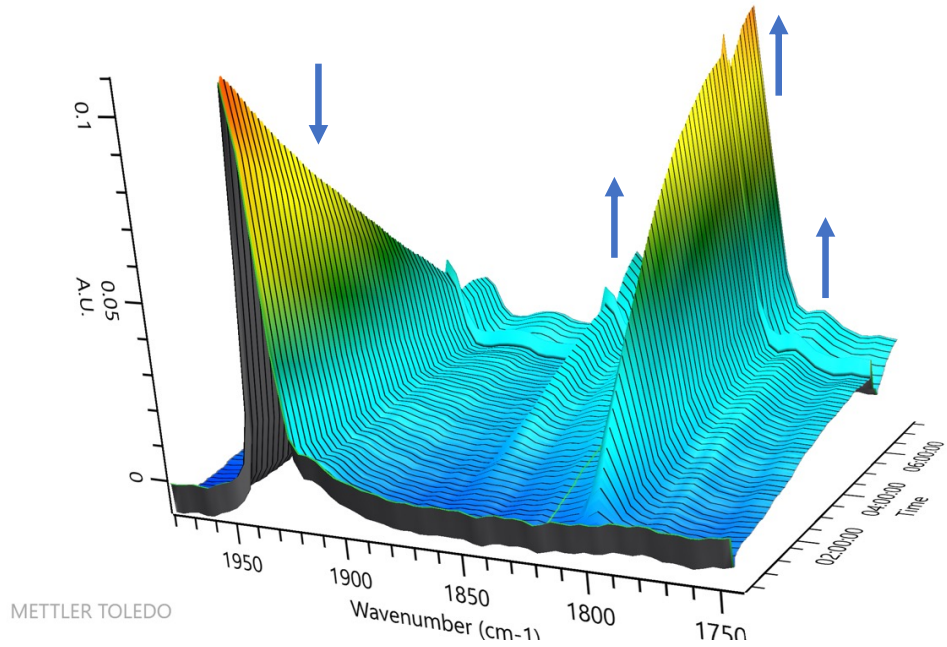

Figure S24. In situ infrared spectrum recorded in pentane of *trans*-[$Cr(N_2)_2(dmpe)_2$] (**2**) with 1 atm of CO. **2** converts to *trans*-[$Cr(CO)_2(dmpe)_2$] ***trans*-2-CO** (ν_{CO} = 1798 cm^{-1}) and *cis*-[$Cr(CO)_2(dmpe)_2$] ***cis*-2-CO** (ν_{CO} = 1857, 1776 cm^{-1}); reaction time of 6 h shown.

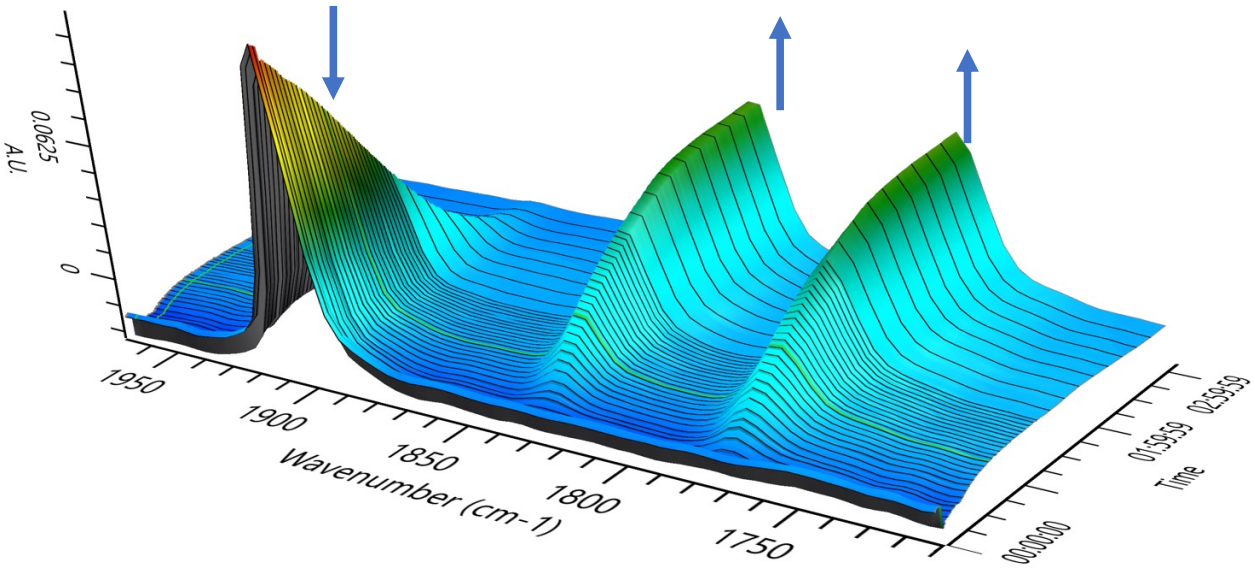

Figure S25. In situ infrared spectrum of *trans*-[Cr(N$_2$)$_2$(depe)$_2$] (**1**) with 1 atm of CO recorded in THF. **1** converts to *cis*-[Cr(CO)$_2$(depe)$_2$] ***cis*-1-CO** in 3 h (ν_{CO} = 1829, 1768 cm^{-1}).

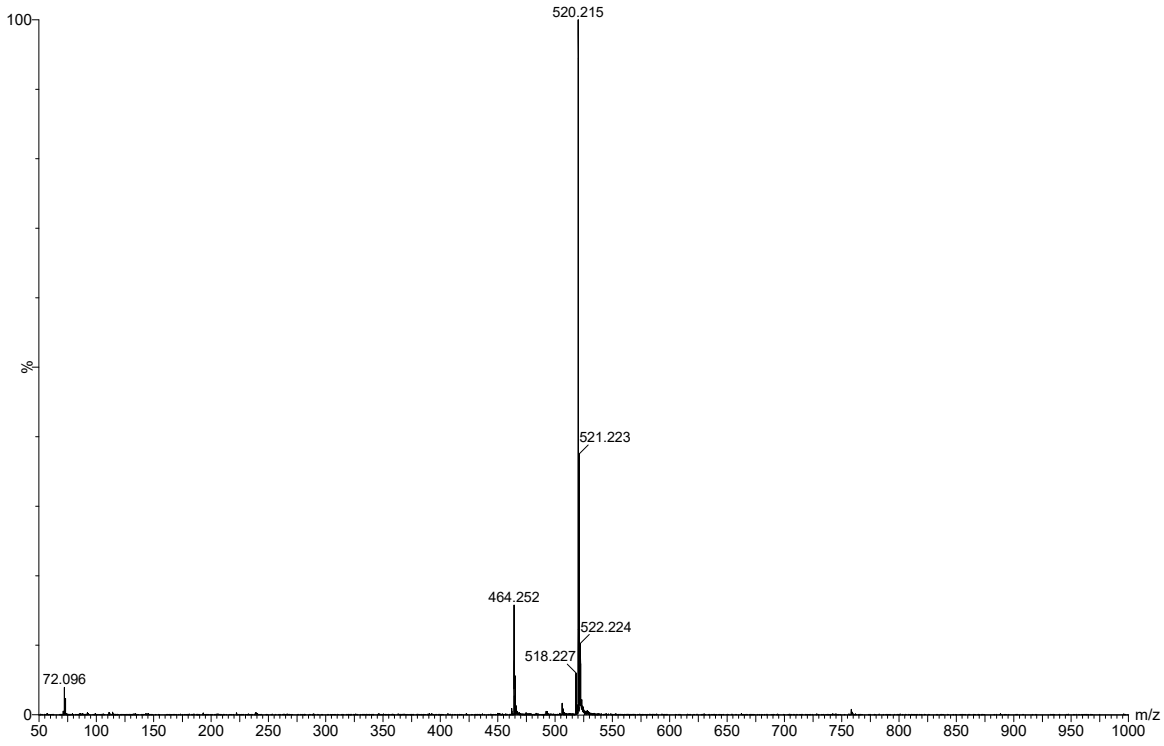

Figure S26. Full LIFDI-MS spectrum of *trans*-[Cr(N$_2$)$_2$(depe)$_2$] (**1**) recorded in THF.

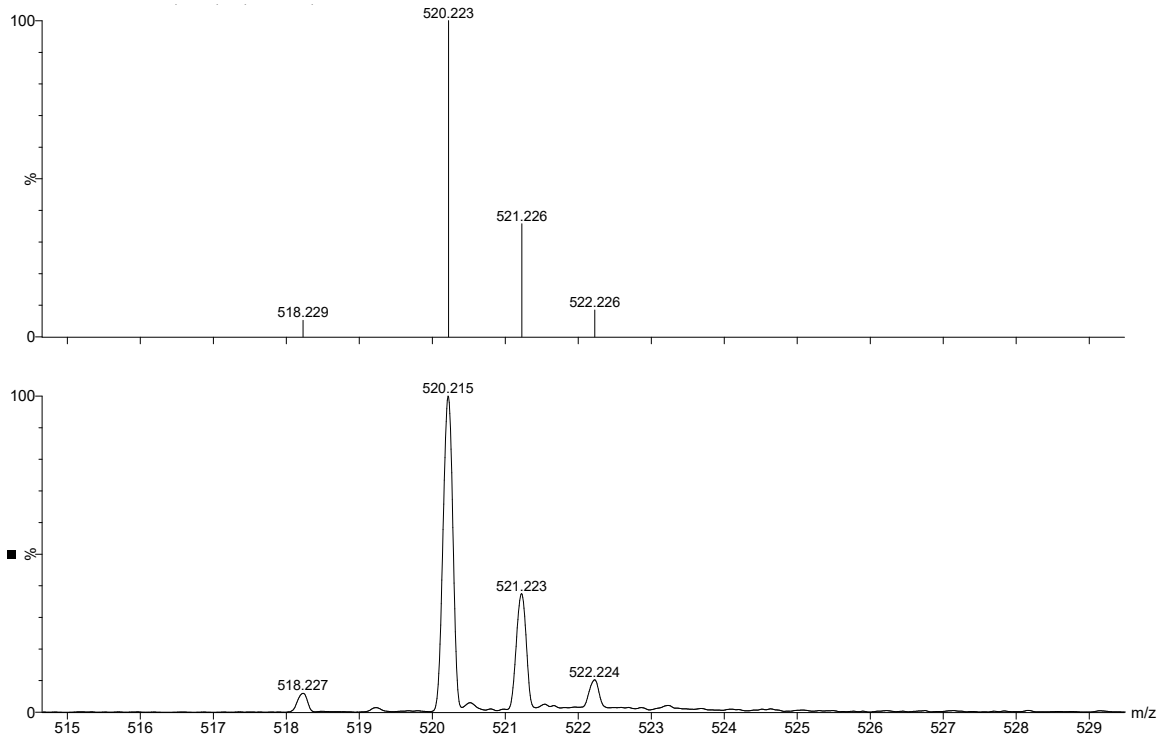

Figure S27. LIFDI-MS spectrum of *trans*-[$Cr(N_2)_2(depe)_2$] (**1**) recorded in THF showing *m/z* 520 (bottom) and the calculated isotope pattern (top).

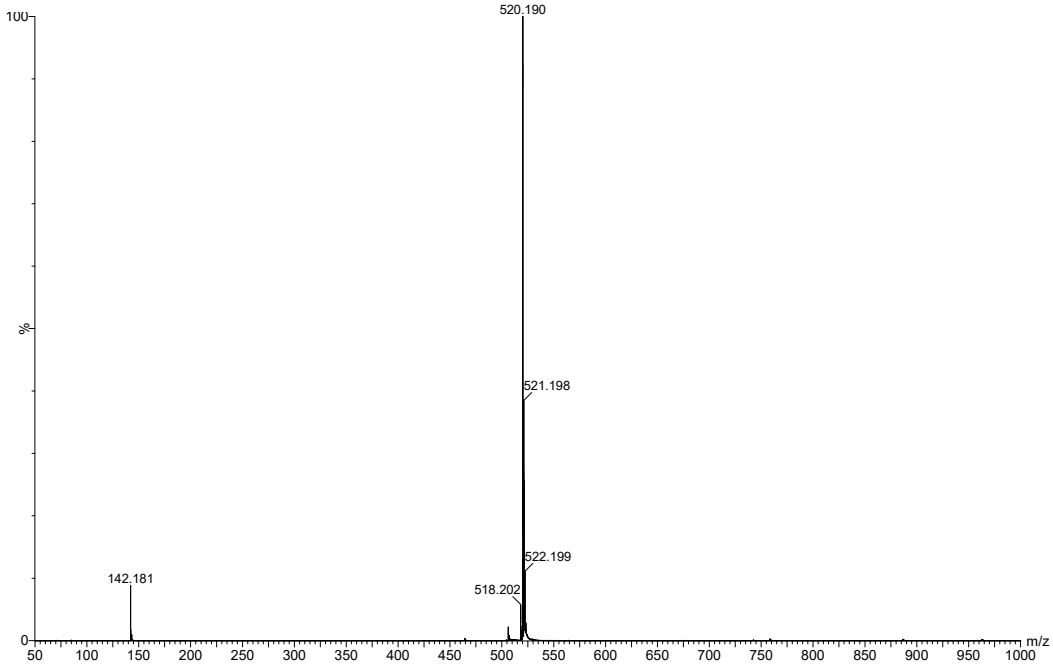

Figure S28. LIFDI-MS full spectrum of *cis*-[$Cr(CO)_2(depe)_2$] ***cis*-1-CO** recorded in THF.

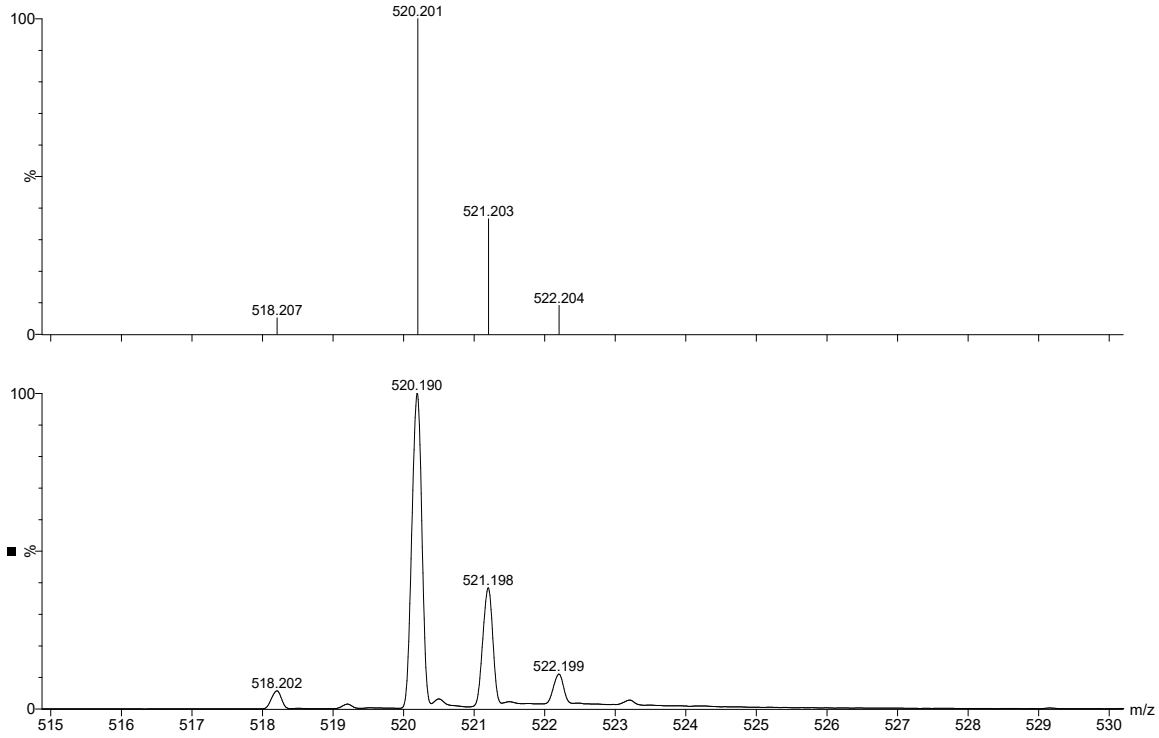

Figure S29. LIFDI-MS of *cis*-[Cr(CO)$_2$(depe)$_2$] ***cis*-1-CO** recorded in THF.

Table S1. Tabulated results for [Cr] catalyzed N_2 reduction experiments.

	Catalyst	Alcohol	NH_3 equiv/Cr	N_2H_4 equiv/Cr	Total Fixed N_2	H_2 equiv/Cr	rxn time (h)	SmI_2 equiv/ Cr	ROH equiv/Cr
1	No Cat.	$(CH_2OH)_2$	0.0	0.0	0.0	157.6	48	583	1166
2	**2**	$(CH_2OH)_2$	3.2	1.7	4.9	180.0	99	146	146
3	**2**	$(CH_2OH)_2$	14.0	6.2	20.2	217.0	48	583	1166
4	**2**	$(CH_2OH)_2$	16.0	3.5	19.5	240.0	48	583	1166
5	**2**	$(CH_2OH)_2$	12.6	3.9	16.4	198.3	48	583	1166
6	**2**	$(CH_2OH)_2$	15.7	9.9	25.6	101.0	48	583	1166
		average	14.6 ± 1.6	5.9 ± 2.9	20.5 ± 3.8	189.1			
7	**2**	H_2O	3.2	4.3	7.5	22.2	48	583	1166
8	**2**	H_2O	5.1	5.9	10.9	276.0	3	583	10000
9	**2**	H_2O	3.0	6.7	9.7	211.0	3	583	20000
10 [a]	2	$(CH_2OH)_2$ and 519 equiv dmpe	0.6	3.8	4.4	89	48	583	1166
11[b]	**2**	$(CH_2OH)_2$	6.5	5.9	12.4	57.0	48	583	1166
12[b]	**2**	$(CH_2OH)_2$	5.8	7.0	12.8	51.0	48	583	1166
		average	6.2 ± 0.5	6.4 ± 0.8	12.6 ± 0.3	54.0			
13[c]	**2**	$(CH_2OH)_2$	3.7	7.0	10.7	147.0	48	583	1166
14[c]	**2**	$(CH_2OH)_2$	5.0	6.2	11.2	52.0	48	583	1166
		average	4.4 ± 0.9	6.6 ± 0.6	11.0 ± 0.4	99.5			
15	**2**	1:1 $(CH_2OH)_2$ and H_2O	1.3	1.8	3.0	60.0	48	583	583:583
16	**2** (run with 1 atm $^{15}N_2$)	$(CH_2OH)_2$	7.3	9.9	17.2	93	48	583	1166
17	$CrCl_2(dmpe)_2$ (**2-Cl**)	$(CH_2OH)_2$	15.5	6.3	21.8	221.0	48	583	1166
18	$CrCl_2(dmpe)_2$ (**2-Cl**)	$(CH_2OH)_2$	11.6	5.4	17.0	200.0	48	583	1166
		average	13.5 ± 2.8	5.9 ± 0.6	19.4 ± 3.4	210.5			
19	**1**	$(CH_2OH)_2$	5.3	5.0	10.3	271.0	100	583	1166
20	**1**	$(CH_2OH)_2$	4.2	2.0	6.2	181.0	120	583	1166
21	**1**	$(CH_2OH)_2$	4.4	4.9	9.3	284.0	141	583	1166
		average	4.6 ± 0.6	4.0 ± 2.7	8.6 ± 2.1	245.3			
22	**1**	$(CH_2OH)_2$	3.2	2.6	5.8	185.0	24	583	1166
23	**1**	$(CH_2OH)_2$	4.1	2.2	6.3	188.0	48	583	1166
24	**1**	$(CH_2OH)_2$	4.6	0.9	5.5	--	48	583	1166
25	**1**	$(CH_2OH)_2$	3.7	1.4	5.2	177.7	48	583	1166
26	**1**	$(CH_2OH)_2$	2.6	0.2	2.8	169.7	48	583	1166
		average	3.7 ± 0.9	1.4 ± 0.8	4.9 ± 1.5	178.5			
27	**1**	H_2O	1.4	0.7	2.1	14.4	48	583	1000
28	**1**	H_2O	0.6	1.9	2.5	23.1	48	583	1166
29	**1**	H_2O	3.2	0.6	3.8	266.4	28	583	10000
30	$CrCl_2(depe)_2$ (**1-Cl**)	$(CH_2OH)_2$	1.2	0.9	2.1	227.4	48	583	1166

[a]performed using 0.25 μmol catalyst [b] THF reaction solvent contained 25 ppm of H_2O. [c] THF reaction solvent contained 250 ppm of H_2O. Experiments performed using 0.6 μmol catalyst in 15.0 mL THF at 25 °C under 1 atm N_2.

General procedure for X-ray diffraction studies and structure refinement details for complexes 1 and 2.

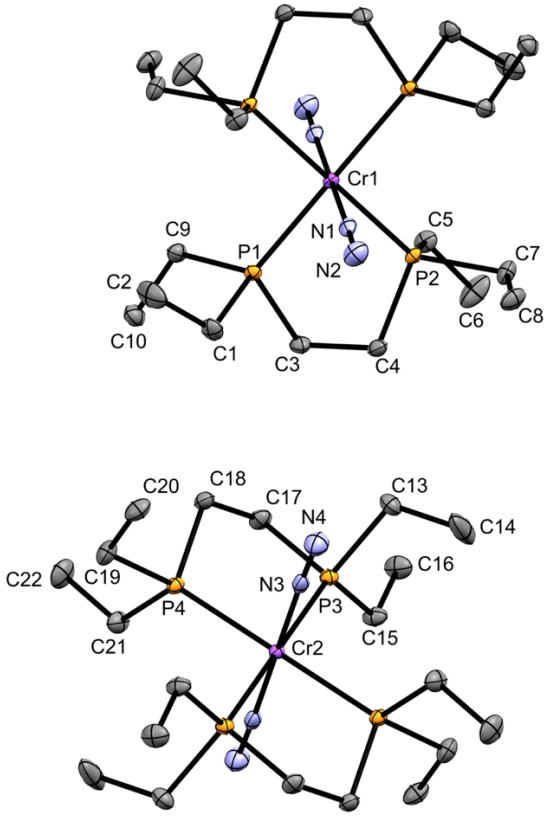

X-Ray crystal structure of *trans*-[$Cr(N_2)_2(depe)_2$] (**1**) with atom labelling. Thermal ellipsoids are drawn at 50% probability. Hydrogen atoms are omitted for clarity.

Crystallographic data. The X-ray diffraction data were measured at 100 K on a Bruker SMART APEX II CCD area detector system equipped with a graphite monochromator and a Mo Kα fine-focus sealed tube operated at 1.2 kW power (40 kV, 30 mA). A red rectangular prism of $Cr(N_2)_2(depe)_2$ of approximate dimensions 0.543 × 0.437 × 0.306 mm^3 was glued to a MiTeGen micromount using Paratone N oil. The detector was placed at a distance of 5.12 cm from the crystal during the data collection.

A series of narrow frames of data were collected with an exposure time of 10 s per frame. The frames were integrated with the Bruker SAINT Software package[8] using a narrow-frame integration algorithm. The integration of the data using a triclinic unit cell yielded a total of 879154 reflections in the θ range of 1.262 to 33.728° of which 10628 were independent with $I \geq 2\sigma(I)$ (R_{int} = 0.0262). The data were corrected for absorption effects by the multi-scan method (SADABS). The structure was solved and refined by the direct methods using the Bruker SHELXTL (V2017.3-0) Software Package.[8,9] All non-hydrogen atoms were located in successive Fourier maps. The asymmetric unit consists of two well-ordered and well-separated $Cr(N_2)_2(depe)_2$ compound molecules. All non-hydrogen atoms were refined anisotropically. All H atoms were also located in successive Fourier maps and were refined isotropically.

The chemically identical $Cr(N_2)_2(depe)_2$ compound molecules share nearly identical structural features. Their crystallographic uniqueness appears to arise from their packing. The CrP_4 chelate planes in the two molecules are strictly planar as the plane is dissected by a two-fold axis and a two-fold planes of symmetry also passes through it. The CrP_4 planes have a dihedral angle of 69.019 (6)°. Two N_2 ligands coordinate to the central Cr(0) atom as monodentate ligands with the angle between the ligands and the CrP_4 plane being nearly 90° in both molecules.

The final refinement parameters are R_1 = 0.0290 and wR_2 = 0.0696 for data with $F > 4\sigma(F)$ giving the data to parameter ratio of 23. The refinement data for all data are R_1 = 0.0346 and wR_2 = 0.0736.

Crystal data and structure refinement for *trans*-[Cr(N_2)$_2$(depe)$_2$] (**1**).

Empirical formula	C20 H48 Cr N4 P4	
Formula weight	520.50	
Temperature	100(2) K	
Wavelength	0.71073 Å	
Crystal system	Triclinic	
Space group	P-1	
Unit cell dimensions	a = 8.2082(4) Å	α = 104.253(2)°.
	b = 10.3281(5) Å	β = 90.264(2)°.
	c = 16.6727(8) Å	γ = 102.507(2)°.
Volume	1334.90(11) Å^3	
Z	2	
Density (calculated)	1.295 g/cm^3	
Absorption coefficient	0.683 mm^{-1}	
F(000)	560	
Crystal size	0.543 × 0.437 × 0.306 mm^3	
Theta range for data collection	1.262 to 33.728°.	
Index ranges	$-12 \le h \le 12$, $-16 \le k \le 16$, $-26 \le l \le 26$	
Reflections collected	87915	
Independent reflections	10628 [R(int) = 0.0262]	
Completeness to theta = 25.242°	99.9 %	
Absorption correction	Semi-empirical from equivalents	
Max. and min. transmission	0.7469 and 0.6736	
Refinement method	Full-matrix least-squares on F^2	
Data / restraints / parameters	10628 / 0 / 457	
Goodness-of-fit on F^2	1.084	
Final R indices [I>2sigma(I)]	R1 = 0.0290, wR2 = 0.0696	
R indices (all data)	R1 = 0.0346, wR2 = 0.0736	
Extinction coefficient	n/a	
Largest diff. peak and hole	1.116 and -0.609 e.Å^{-3}	

Bond lengths [Å] and angles [°] for *trans*-[$Cr(N_2)_2(depe)_2$].

Cr(1)-N(1)	1.9081(10)
Cr(1)-N(1)#1	1.9081(10)
Cr(1)-P(2)	2.3249(3)
Cr(1)-P(2)#1	2.3249(3)
Cr(1)-P(1)	2.3343(3)
Cr(1)-P(1)#1	2.3343(3)
P(1)-C(9)	1.8450(10)
P(1)-C(1)	1.8490(11)
P(1)-C(3)	1.8648(10)
P(2)-C(7)	1.8467(11)
P(2)-C(5)	1.8505(10)
P(2)-C(4)	1.8517(11)
N(1)-N(2)	1.1003(14)
Cr(2)-N(3)	1.9008(10)
Cr(2)-N(3)#2	1.9008(10)
Cr(2)-P(4)	2.3346(3)
Cr(2)-P(4)#2	2.3346(3)
Cr(2)-P(3)	2.3425(3)
Cr(2)-P(3)#2	2.3425(3)
P(3)-C(15)	1.8451(11)
P(3)-C(13)	1.8501(11)
P(3)-C(17)	1.8622(11)
P(4)-C(19)	1.8457(11)
P(4)-C(21)	1.8509(11)
P(4)-C(18)	1.8512(11)
N(3)-N(4)	1.1069(14)
C(1)-C(2)	1.5157(18)
C(1)-H(1A)	0.962(18)
C(1)-H(1B)	0.93(2)
C(2)-H(2A)	0.93(2)
C(2)-H(2B)	0.91(2)
C(2)-H(2C)	0.99(2)
C(3)-C(4)	1.5291(15)

C(3)-H(3A)	0.982(17)
C(3)-H(3B)	0.968(17)
C(4)-H(4A)	0.977(18)
C(4)-H(4B)	0.953(17)
C(5)-C(6)	1.5140(16)
C(5)-H(5A)	0.942(19)
C(5)-H(5B)	0.947(19)
C(6)-H(6A)	0.97(2)
C(6)-H(6B)	1.02(3)
C(6)-H(6C)	0.86(3)
C(7)-C(8)	1.5243(16)
C(7)-H(7A)	0.968(18)
C(7)-H(7B)	0.979(19)
C(8)-H(8A)	0.95(2)
C(8)-H(8B)	0.937(18)
C(8)-H(8C)	0.96(2)
C(9)-C(10)	1.5259(15)
C(9)-H(9A)	0.986(17)
C(9)-H(9B)	0.961(18)
C(10)-H(10A)	0.969(18)
C(10)-H(10B)	0.978(19)
C(10)-H(10C)	0.971(19)
C(17)-C(18)	1.5316(16)
C(17)-H(17A)	0.968(17)
C(17)-H(17B)	0.949(18)
C(18)-H(18A)	0.976(18)
C(18)-H(18B)	0.942(17)
C(19)-C(20)	1.5225(17)
C(19)-H(19A)	0.971(19)
C(19)-H(19B)	0.971(18)
C(20)-H(20A)	0.96(2)
C(20)-H(20B)	0.964(18)
C(20)-H(20C)	0.97(2)
C(21)-C(22)	1.5211(16)
C(21)-H(21A)	0.93(2)
C(21)-H(21B)	0.94(2)

C(22)-H(22A)	0.99(2)
C(22)-H(22B)	0.94(2)
C(22)-H(22C)	0.95(2)
C(13)-C(14)	1.507(2)
C(13)-H(13A)	0.963(18)
C(13)-H(13B)	0.93(2)
C(14)-H(14A)	0.96(2)
C(14)-H(14B)	0.91(3)
C(14)-H(14C)	0.92(3)
C(15)-C(16)	1.5258(16)
C(15)-H(15A)	0.965(18)
C(15)-H(15B)	0.950(18)
C(16)-H(16A)	0.95(2)
C(16)-H(16B)	0.996(18)
C(16)-H(16C)	0.92(2)

N(1)-Cr(1)-N(1)#1	180.0
N(1)-Cr(1)-P(2)	90.21(3)
N(1)#1-Cr(1)-P(2)	89.79(3)
N(1)-Cr(1)-P(2)#1	89.79(3)
N(1)#1-Cr(1)-P(2)#1	90.21(3)
P(2)-Cr(1)-P(2)#1	180.000(17)
N(1)-Cr(1)-P(1)	89.25(3)
N(1)#1-Cr(1)-P(1)	90.75(3)
P(2)-Cr(1)-P(1)	81.650(9)
P(2)#1-Cr(1)-P(1)	98.350(9)
N(1)-Cr(1)-P(1)#1	90.75(3)
N(1)#1-Cr(1)-P(1)#1	89.25(3)
P(2)-Cr(1)-P(1)#1	98.350(9)
P(2)#1-Cr(1)-P(1)#1	81.650(9)
P(1)-Cr(1)-P(1)#1	180.000(14)
C(9)-P(1)-C(1)	103.12(5)
C(9)-P(1)-C(3)	101.72(5)
C(1)-P(1)-C(3)	97.98(5)
C(9)-P(1)-Cr(1)	119.24(3)
C(1)-P(1)-Cr(1)	119.97(4)

C(3)-P(1)-Cr(1)	111.38(3)
C(7)-P(2)-C(5)	101.35(5)
C(7)-P(2)-C(4)	100.58(5)
C(5)-P(2)-C(4)	100.15(5)
C(7)-P(2)-Cr(1)	126.53(4)
C(5)-P(2)-Cr(1)	115.51(4)
C(4)-P(2)-Cr(1)	108.86(3)
N(2)-N(1)-Cr(1)	178.56(9)
N(3)-Cr(2)-N(3)#2	180.0
N(3)-Cr(2)-P(4)	90.59(3)
N(3)#2-Cr(2)-P(4)	89.41(3)
N(3)-Cr(2)-P(4)#2	89.41(3)
N(3)#2-Cr(2)-P(4)#2	90.59(3)
P(4)-Cr(2)-P(4)#2	180.000(11)
N(3)-Cr(2)-P(3)	89.29(3)
N(3)#2-Cr(2)-P(3)	90.71(3)
P(4)-Cr(2)-P(3)	81.583(10)
P(4)#2-Cr(2)-P(3)	98.417(10)
N(3)-Cr(2)-P(3)#2	90.71(3)
N(3)#2-Cr(2)-P(3)#2	89.29(3)
P(4)-Cr(2)-P(3)#2	98.417(10)
P(4)#2-Cr(2)-P(3)#2	81.583(10)
P(3)-Cr(2)-P(3)#2	180.0
C(15)-P(3)-C(13)	102.85(5)
C(15)-P(3)-C(17)	101.88(5)
C(13)-P(3)-C(17)	97.26(5)
C(15)-P(3)-Cr(2)	119.92(4)
C(13)-P(3)-Cr(2)	120.25(4)
C(17)-P(3)-Cr(2)	111.01(4)
C(19)-P(4)-C(21)	100.54(6)
C(19)-P(4)-C(18)	101.04(5)
C(21)-P(4)-C(18)	100.29(5)
C(19)-P(4)-Cr(2)	125.62(4)
C(21)-P(4)-Cr(2)	116.91(4)
C(18)-P(4)-Cr(2)	108.72(4)
N(4)-N(3)-Cr(2)	178.25(9)

C(2)-C(1)-P(1)	115.27(9)
C(2)-C(1)-H(1A)	110.9(11)
P(1)-C(1)-H(1A)	106.5(11)
C(2)-C(1)-H(1B)	109.3(13)
P(1)-C(1)-H(1B)	108.3(13)
H(1A)-C(1)-H(1B)	106.2(16)
C(1)-C(2)-H(2A)	110.3(13)
C(1)-C(2)-H(2B)	113.1(15)
H(2A)-C(2)-H(2B)	109.8(19)
C(1)-C(2)-H(2C)	112.9(14)
H(2A)-C(2)-H(2C)	108.1(19)
H(2B)-C(2)-H(2C)	102(2)
C(4)-C(3)-P(1)	108.08(7)
C(4)-C(3)-H(3A)	111.2(10)
P(1)-C(3)-H(3A)	110.0(10)
C(4)-C(3)-H(3B)	110.4(10)
P(1)-C(3)-H(3B)	108.0(10)
H(3A)-C(3)-H(3B)	109.1(14)
C(3)-C(4)-P(2)	107.69(7)
C(3)-C(4)-H(4A)	113.2(10)
P(2)-C(4)-H(4A)	111.8(10)
C(3)-C(4)-H(4B)	110.8(10)
P(2)-C(4)-H(4B)	105.3(10)
H(4A)-C(4)-H(4B)	107.8(14)
C(6)-C(5)-P(2)	118.77(8)
C(6)-C(5)-H(5A)	110.2(11)
P(2)-C(5)-H(5A)	105.2(11)
C(6)-C(5)-H(5B)	109.7(12)
P(2)-C(5)-H(5B)	108.0(12)
H(5A)-C(5)-H(5B)	103.9(16)
C(5)-C(6)-H(6A)	111.6(12)
C(5)-C(6)-H(6B)	110.1(14)
H(6A)-C(6)-H(6B)	105.1(18)
C(5)-C(6)-H(6C)	110.6(17)
H(6A)-C(6)-H(6C)	111(2)
H(6B)-C(6)-H(6C)	108(2)

C(8)-C(7)-P(2)	113.92(8)
C(8)-C(7)-H(7A)	108.7(11)
P(2)-C(7)-H(7A)	108.6(11)
C(8)-C(7)-H(7B)	112.6(11)
P(2)-C(7)-H(7B)	106.9(11)
H(7A)-C(7)-H(7B)	105.6(15)
C(7)-C(8)-H(8A)	109.9(12)
C(7)-C(8)-H(8B)	111.7(11)
H(8A)-C(8)-H(8B)	107.6(16)
C(7)-C(8)-H(8C)	111.5(12)
H(8A)-C(8)-H(8C)	107.7(16)
H(8B)-C(8)-H(8C)	108.3(16)
C(10)-C(9)-P(1)	118.31(8)
C(10)-C(9)-H(9A)	109.9(10)
P(1)-C(9)-H(9A)	105.7(10)
C(10)-C(9)-H(9B)	109.7(11)
P(1)-C(9)-H(9B)	104.7(11)
H(9A)-C(9)-H(9B)	108.0(14)
C(9)-C(10)-H(10A)	111.3(11)
C(9)-C(10)-H(10B)	111.2(11)
H(10A)-C(10)-H(10B)	108.2(15)
C(9)-C(10)-H(10C)	110.5(11)
H(10A)-C(10)-H(10C)	106.4(15)
H(10B)-C(10)-H(10C)	109.1(15)
C(18)-C(17)-P(3)	107.45(7)
C(18)-C(17)-H(17A)	111.3(10)
P(3)-C(17)-H(17A)	109.9(10)
C(18)-C(17)-H(17B)	110.2(11)
P(3)-C(17)-H(17B)	107.9(11)
H(17A)-C(17)-H(17B)	110.0(15)
C(17)-C(18)-P(4)	107.44(7)
C(17)-C(18)-H(18A)	112.6(11)
P(4)-C(18)-H(18A)	113.3(11)
C(17)-C(18)-H(18B)	111.1(11)
P(4)-C(18)-H(18B)	105.8(11)
H(18A)-C(18)-H(18B)	106.4(15)

C(20)-C(19)-P(4)	113.30(8)
C(20)-C(19)-H(19A)	109.2(11)
P(4)-C(19)-H(19A)	109.3(11)
C(20)-C(19)-H(19B)	109.9(11)
P(4)-C(19)-H(19B)	110.0(11)
H(19A)-C(19)-H(19B)	104.7(15)
C(19)-C(20)-H(20A)	110.2(13)
C(19)-C(20)-H(20B)	111.8(10)
H(20A)-C(20)-H(20B)	108.4(16)
C(19)-C(20)-H(20C)	111.3(12)
H(20A)-C(20)-H(20C)	106.9(17)
H(20B)-C(20)-H(20C)	108.0(15)
C(22)-C(21)-P(4)	118.57(8)
C(22)-C(21)-H(21A)	108.8(13)
P(4)-C(21)-H(21A)	108.0(13)
C(22)-C(21)-H(21B)	108.7(12)
P(4)-C(21)-H(21B)	107.1(12)
H(21A)-C(21)-H(21B)	104.8(17)
C(21)-C(22)-H(22A)	111.9(12)
C(21)-C(22)-H(22B)	114.2(14)
H(22A)-C(22)-H(22B)	108.2(18)
C(21)-C(22)-H(22C)	108.8(13)
H(22A)-C(22)-H(22C)	107.5(17)
H(22B)-C(22)-H(22C)	105.9(19)
C(14)-C(13)-P(3)	115.51(10)
C(14)-C(13)-H(13A)	111.2(11)
P(3)-C(13)-H(13A)	107.8(11)
C(14)-C(13)-H(13B)	110.0(13)
P(3)-C(13)-H(13B)	107.4(13)
H(13A)-C(13)-H(13B)	104.3(16)
C(13)-C(14)-H(14A)	111.8(13)
C(13)-C(14)-H(14B)	110.6(18)
H(14A)-C(14)-H(14B)	105(2)
C(13)-C(14)-H(14C)	114.0(16)
H(14A)-C(14)-H(14C)	106(2)
H(14B)-C(14)-H(14C)	109(2)

C(16)-C(15)-P(3)	118.62(8)
C(16)-C(15)-H(15A)	109.6(11)
P(3)-C(15)-H(15A)	106.8(11)
C(16)-C(15)-H(15B)	110.2(11)
P(3)-C(15)-H(15B)	104.7(11)
H(15A)-C(15)-H(15B)	106.1(15)
C(15)-C(16)-H(16A)	110.0(12)
C(15)-C(16)-H(16B)	111.5(11)
H(16A)-C(16)-H(16B)	109.4(15)
C(15)-C(16)-H(16C)	112.4(12)
H(16A)-C(16)-H(16C)	105.5(17)
H(16B)-C(16)-H(16C)	108.0(16)

Symmetry transformations used to generate equivalent atoms:
#1 -x,-y,-z #2 -x+1,-y,-z+1

Torsion angles [°] for *trans*-[$Cr(N_2)_2(depe)_2$].

P(1)-C(3)-C(4)-P(2)	-48.95(8)
P(3)-C(17)-C(18)-P(4)	-51.19(8)

Symmetry transformations used to generate equivalent atoms:
#1 -x,-y,-z #2 -x+1,-y,-z+1

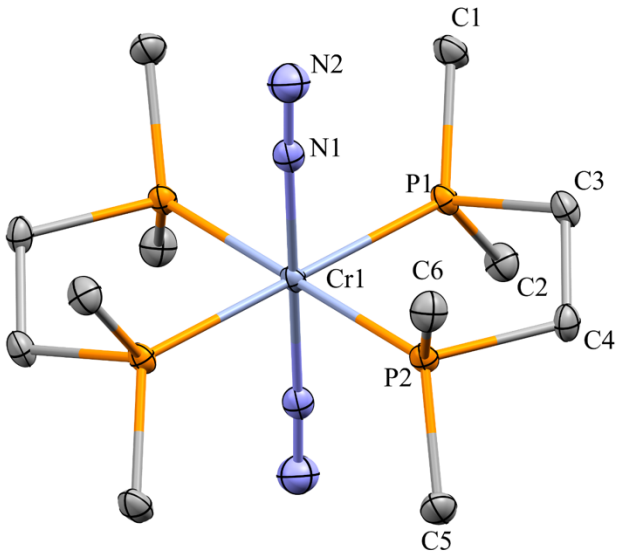

X-Ray crystal structure of *trans*-[$Cr(N_2)_2(dmpe)_2$] (**2**) with atom labelling. Thermal ellipsoids are drawn at 50% probability. Hydrogen atoms are omitted for clarity.

A red, plate-like specimen of $C_{12}H_{32}CrN_4P_4$, approximate dimensions 0.080 mm × 0.140 mm × 0.220 mm, was used for the X-ray crystallographic analysis. The X-ray intensity data were measured (λ = 0.71073 Å) on a Bruker D8 Venture Duo X-ray diffractometer equipped with a CMOS IμS 3.0 Mo source and a PHOTON detector. A total of 1458 frames were collected. The total exposure time was 1.32 hours. The frames were integrated with the Bruker SAINT software package using a narrow-frame algorithm. The integration of the data using a triclinic unit cell yielded a total of 9152 reflections to a maximum θ angle of 29.58° (0.72 Å resolution), of which 2749 were independent (average redundancy 3.329, completeness = 97.2%, R_{int} = 5.52%, R_{sig} = 5.98%) and 2200 (80.03%) were greater than $2\sigma(F^2)$. The final cell constants of a = 7.4075(14) Å, b = 8.6330(17) Å, c = 8.9332(19) Å, α = 104.558(6)°, β = 105.008(6)°, γ = 103.613(7)°, volume = 505.73(18) Å^3, are based upon the refinement of the XYZ-centroids of 3208 reflections above 2 $\sigma(I)$ with 5.864° < 2θ < 66.34°. Data was corrected for absorption effects using the multi-scan

method (SADABS). The ratio of minimum to maximum apparent transmission was 0.763. The calculated minimum and maximum transmission coefficients (based on crystal size) are 0.8300 and 0.9330.

The structure was solved and refined using the Bruker SHELXTL Software Package[9,10], using the space group *P-1*, with $Z = 1$ for the formula unit, $C_{12}H_{32}CrN_4P_4$. The non-hydrogen atoms were located in successive Fourier maps and refined anisotropically. The H atoms were also located in the Fourier maps and refined isotropically. The asymmetric unit contains a half of the $Cr(N_2)_2(dmpe)_2$ compound molecule. The final anisotropic full-matrix least-squares refinement on F^2 with 162 variables converged at $R_1 = 3.78\%$, for the observed data and $wR_2 = 7.66\%$ for all data. The goodness-of-fit was 1.067. The largest peak in the final difference electron density synthesis was 0.480 $e^-/Å^3$ and the largest hole was -0.432 $e^-/Å^3$ with an RMS deviation of 0.085 $e^-/Å^3$. On the basis of the final model, the calculated density was 1.341 g/cm^3 and F(000), 216 e^-.

Sample and crystal data for *trans*-[$Cr(N_2)_2(dmpe)_2$] (**2**).

Chemical formula	$C_{12}H_{32}CrN_4P_4$	
Formula weight	408.29 g/mol	
Temperature	100(2) K	
Wavelength	0.71073 Å	
Crystal size	0.080 × 0.140 × 0.220 mm	
Crystal habit	red plate	
Crystal system	triclinic	
Space group	*P -1*	
Unit cell dimensions	a = 7.4075(14) Å	α = 104.558(6)°
	b = 8.6330(17) Å	β = 105.008(6)°
	c = 8.9332(19) Å	γ = 103.613(7)°
Volume	505.73(18) $Å^3$	
Z	1	
Density (calculated)	1.341 g/cm^3	
Absorption coefficient	0.881 mm^{-1}	
F(000)	216	
Theta range for data collection	2.57 to 29.58°	
Index ranges	$-10 \leq h \leq 10$, $-11 \leq k \leq 11$, $-12 \leq l \leq 12$	
Reflections collected	9152	
Independent reflections	2749 [R_{int} = 0.0552]	
Coverage of independent reflections	97.2%	
Absorption correction	Multi-Scan	
Max. and min. transmission	0.9330 and 0.8300	
Structure solution technique	direct methods	
Structure solution program	XT, VERSION 2018/2	
Refinement method	Full-matrix least-squares on F^2	

Refinement program	SHELXL-2019/1 (Sheldrick, 2019)	
Function minimized	$\Sigma w(F_o^2 - F_c^2)^2$	
Data / restraints / parameters	2749 / 0 / 162	
Goodness-of-fit on F^2	1.067	
Final *R* indices	2200 data; $I > 2\sigma(I)$	$R_1 = 0.0378$, $wR_2 = 0.0720$
	all data	$R_1 = 0.0523$, $wR_2 = 0.0766$
Weighting scheme	$w = 1/[\sigma^2(F_o^2) + (0.0291P)^2]$ where $P = (F_o^2 + 2F_c^2)/3$	
Largest diff. peak and hole	0.480 and -0.432 eÅ^{-3}	
R.M.S. deviation from mean	0.085 eÅ^{-3}	

Bond lengths (Å) for *trans*-[$Cr(N_2)_2(dmpe)_2$]

Cr1-N1	1.8862(17)	Cr1-N1#1	1.8862(17)
Cr1-P1	2.2895(6)	Cr1-P1#1	2.2895(6)
Cr1-P2	2.2976(6)	Cr1-P2#1	2.2976(6)
N1-N2	1.110(2)	P1-C2	1.829(2)
P1-C1	1.8334(19)	P1-C3	1.8555(19)
P2-C5	1.831(2)	P2-C6	1.834(2)
P2-C4	1.8610(19)	C3-C4	1.519(3)

Symmetry transformations used to generate equivalent atoms:

#1 -x+1, -y+1, -z+1

Bond angles (°) for *trans*-[Cr(N_2)$_2$(dmpe)$_2$].

N1#1-Cr1-N1	180.00(10)	N1#1-Cr1-P1	92.12(5)
N1-Cr1-P1	87.88(5)	N1#1-Cr1-P1#1	87.88(5)
N1-Cr1-P1#1	92.12(5)	P1-Cr1-P1#1	180.000000
N1#1-Cr1-P2	90.95(5)	N1-Cr1-P2	89.05(5)
P1-Cr1-P2	83.54(2)	P1#1-Cr1-P2	96.46(2)
N1#1-Cr1-P2#1	89.05(5)	N1-Cr1-P2#1	90.95(5)
P1-Cr1-P2#1	96.46(2)	P1#1-Cr1-P2#1	83.54(2)
P2-Cr1-P2#1	180.000000	N2-N1-Cr1	178.20(14)
C2-P1-C1	100.85(10)	C2-P1-C3	101.16(10)
C1-P1-C3	99.87(9)	C2-P1-Cr1	119.36(7)
C1-P1-Cr1	122.79(7)	C3-P1-Cr1	109.25(6)
C5-P2-C6	101.01(10)	C5-P2-C4	100.13(9)
C6-P2-C4	101.20(10)	C5-P2-Cr1	123.10(7)
C6-P2-Cr1	117.36(7)	C4-P2-Cr1	110.72(6)
C4-C3-P1	109.09(13)	C3-C4-P2	109.33(13)

Symmetry transformations used to generate equivalent atoms:

#1 -x+1, -y+1, -z+1

Torsion angles (°) for *trans*-[Cr(N_2)$_2$(dmpe)$_2$].

P1-C3-C4-P2	45.24(16)

References for ESI

1. M. T. Mock, S. Chen, M. O'Hagan, R. Rousseau, W. G. Dougherty, W. S. Kassel and R. M. Bullock, *J. Am. Chem. Soc.*, 2013, **135**, 11493-11496.
2. Y. Ashida, S. Kondo, K. Arashiba, T. Kikuchi, K. Nakajima, S. Kakimoto and Y. Nishibayashi, *Synthesis*, 2019, **51**, 3792-3795.
3. G. S. Girolami, J. E. Salt, G. Wilkinson, M. Thornton-Pett and M. B. Hursthouse, *J. Am. Chem. Soc.*, 1983, **105**, 5954-5956.
4. A. J. Kendall, S. I. Johnson, R. M. Bullock and M. T. Mock, *J. Am. Chem. Soc.*, 2018, **140**, 2528-2536.
5. G. Ricci, A. Forni, A. Boglia and M. Sonzogni, *Organometallics*, 2004, **23**, 3727-3732.
6. G. W. Watt and J. D. Chrisp, *Anal. Chem.*, 1952, **24**, 2006-2008.
7. P. J. Hill, L. R. Doyle, A. D. Crawford, W. K. Myers and A. E. Ashley, *J. Am. Chem. Soc.*, 2016, **138**, 13521-13524.
8. APEX3 Software Suite V2017.3-0, Bruker AXS Inc.: Madison, WI, 2017.
9. Sheldrick,G.M.,"Crystal structure refinement with SHELXL", *Acta Cryst.* 2015, **C71**, 3-8.
10. APEX4 Software Suite V2022. 1-1, Bruker AXS Inc.: Madison, WI, 2022.